Fabrication of Curli-expressing Biofilm-textile Composites for Self-repairing High-performance Textiles

Anqi (Angie) Cai

Department of Chemical Engineering | McGill University, Montreal

April 2023

A thesis submitted to McGill University in partial fulfillment of the requirements of the degree of

Master of Science (Thesis)

Table of Contents

List of Figures

Chapter 2

Chapter 3

List of Abbreviations

AS	Adsorption
CFU	Colony forming units
DB	Doctor blading
DI water	Deionized water
E. coli	*Escherichia Coli*
ELMs	Engineered Living Materials
EPS	Extracellular polymeric substances
FAS	Fluorinated alkyl silane
FD-POSS	Fluorinated-decyl polyhedral oligomeric silsesquioxane
FESEM	Field-emission scanning electron microscopy
FS-NPs	Fluoroalkyl surface-modified silica nanoparticles
GFP	Green fluorescent protein
HAP	Hydroxyapatite
LB	Lysogeny broth
OV-POSS	Octavinyl-polyhedral oligomeric silsesquioxane
PAL	Palygorskite
PDMS	Polydimethylsiloxane
PEDOT	Poly(3,4-ethylenedioxythiophene)
PFDTES	1H,1H,2H,2H-perfluorodecyltriethoxysilane
PSS	Polystyrenesulfonate
PVDF-HFP	Poly(vinylidene fluoride-hexafluoropropylene)
SEM	Scanning electron microscopy
SRT	Squid ring teeth
TEOS	Tetraethoxysilane
TV-PFOD	Tri-functionality vinyl perfluoro decanol
VF	Vacuum filtration
V-PDMS	Vinyl-terminated polydimethylsiloxane
WVTR	Water vapor transmission rate

Abstract

Textiles displaying improved physical, mechanical and functional properties are desired for clothing, wearable devices, and technical textiles. To minimize the environmentally destructive impacts of textile production and reduce textile waste, textiles that can self-repair defects, and thus have a prolonged lifespan, have been developed by incorporating external repair agents into traditional textiles. However, many reported self-repairing strategies function on limited size scales, require complex chemistries or polluting solvents, and have environmental and health concerns. Instead, biologically-derived repair agents are renewable, biodegradable, and biocompatible, conforming to the requirements of eco-design.

In this work, we incorporated biofilms, formed by *Escherichia coli* (*E. coli*) for surface colonization and protection purposes, into conventional textiles. Biofilms comprise curli fibers expressed and secreted by the bacteria. Curli fibers, which are structurally ordered amyloids, are known for their mechanical strength, stability in harsh environments, self-healing behavior, and genetic tunability. First, we integrated curli-expressing *E. coli* biofilms into common knitted cotton textiles via three facile and scalable fabrication methods – adsorption, doctor blading, and vacuum filtration. To assess the composites' applicability in wearables, we studied their wettability, breathability, and mechanical properties. Then, we investigated the self-repairing ability of the composites and repaired composites cut in half by patching and welding. To confirm the quality of self-repair, we quantified the adhesion strength of the patched composites using single lap shear tests, and the breaking stress of the welded ones with tensile tests.

We observed that the different fabrication methods resulted in different morphologies of the biofilm-textile composites. The introduction of the biofilm layer modified the textiles' surface wettability, maintained their water vapor transmission rates, and enhanced their mechanical

properties. Notably, biofilm adsorption increased the textiles' elastic modulus by an average of ~120%, while composites with vacuum-filtered biofilm coating were ~140% more extensible at break than the original textiles. We demonstrated that the biofilm coating formed with either of the three methods imparted a water-induced self-repairing ability to the textiles, which enabled the composites to effectively repair centimeter-sized damages. We attribute this self-repairing ability to the curli's self-assembly and network formation. When examining the mechanical failure of the repaired composites, we saw that both the cohesion and the adhesion quality of the biofilm layer contributed to the overall self-repairing performance of biofilm-textile composites. Our work provides a simple, scalable, and sustainable route to fabricate durable, high-performance textiles. When combining such fabrication techniques with biofilms' living properties and genetic customizability, more novel and smart functions can be displayed through the composites to redefine the potency of future textiles.

Résumé

Les textiles présentant des propriétés physiques, mécaniques et fonctionnelles améliorées sont recherchés pour les vêtements, les dispositifs portables et les textiles techniques. Pour minimiser les impacts de la production textile sur l'environnement et réduire les déchets textiles, des textiles capables d'autoréparer ses défauts et donc d'avoir une durée de vie prolongée ont été développés en incorporant des agents de réparation externes dans les textiles traditionnels. Cependant, de nombreuses stratégies d'autoréparation rapportées fonctionnent sur des échelles de taille limitées, nécessitent des produits chimiques complexes ou des solvants polluants, et présentent des problèmes environnementaux et sanitaires. Au contraire, les agents de réparation d'origine biologique sont renouvelables, biodégradables et biocompatibles, et respectent les exigences de l'écoconception.

Dans ce travail, nous avons incorporé des biofilms, qui sont formés par *Escherichia coli* (*E. coli*) à des fins de colonisation de surface et de protection, dans des textiles conventionnels. Les biofilms comprennent des fibres curli exprimées et sécrétées par les bactéries. Les fibres curli, qui sont des amyloïdes ordonnées structurellement, sont connues pour leur résistance mécanique, leur stabilité dans des conditions environnementales hostiles, leur comportement d'autoguérison et leur fonctionnalisation génétique. Dans un premier temps, nous avons intégré des biofilms d'*E. coli* exprimant des fibres curli dans des textiles de coton tricotés communs par le biais de trois méthodes de fabrication faciles et évolutives : l'adsorption, le raclage et la filtration sous vide. Pour évaluer l'applicabilité des composites aux vêtements, nous avons étudié leur mouillabilité, leur respirabilité et leurs propriétés mécaniques. Nous avons ensuite étudié la capacité d'autoréparation des composites et réparé les composites coupés en deux par rapiéçage et soudage. Pour confirmer la qualité de l'autoréparation, nous avons quantifié la force d'adhésion des composites rapiécés à

l'aide de tests de cisaillement à simple recouvrement et la contrainte de rupture des composites soudés à l'aide de tests de traction.

Nous avons observé que les différentes méthodes de fabrication ont donné lieu à différentes morphologies des composites biofilm-textile. De plus, l'introduction de la couche de biofilm a modifié la mouillabilité de la surface des textiles, maintenu leur taux de transmission de la vapeur d'eau et amélioré leurs propriétés mécaniques. Notamment, l'adsorption du biofilm a augmenté en moyenne le module élastique des textiles de ~120%, tandis que les composites avec un revêtement de biofilm filtré sous vide étaient ~140% plus extensibles à la rupture que les textiles originaux. Nous avons démontré que le revêtement de biofilm formé par l'une des trois méthodes a conféré aux textiles une capacité d'autoréparation induite par l'eau, ce qui a permis aux composites de réparer efficacement des dommages de taille centimétrique. Nous attribuons ce phénomène à l'autoassemblage et de la formation de réseaux des fibres curli. En examinant la défaillance mécanique des composites réparés, nous avons constaté que la cohésion et la qualité de l'adhésion de la couche de biofilm ont contribué à la performance d'autoréparation des composites biofilm-textile. Notre travail fournit une voie simple, évolutive et durable pour fabriquer des textiles durables et à haute performance. En combinant ces techniques de fabrication avec les propriétés vivantes et la personnalisation génétique des biofilms, plus de fonctions innovantes et intelligentes peuvent être affichées par les composites pour redéfinir la puissance des textiles du futur.

Acknowledgements

First, I would like to express my deepest appreciation to my supervisor, Dr. Noémie-Manuelle Dorval Courchesne. Thank you for always being such a perfect role model - always replying to my requests very fast, always supporting my random research ideas (although they were sometimes too ambitious), always willing to answer my silly questions, always encouraging me whenever I was stuck, and always recognizing every small achievement of mine. I admired Noémie's enthusiasm for research, attention to detail, outstanding time management skills, and care for our lab. I will never forget when she came to the lab on a Saturday afternoon bringing N95 masks for the lab when we were scared of another wave of COVID-19.

I would also like to thank the co-authors of this work, Dalia Jane Saldanha, Zahra Abdali, and Masoud Aminzare. Thank you for making substantial efforts to kick-start this novel, exciting project, conducting preliminary experiments, training me on the lab equipment, and sharing the workload. I have learned so much from each of you, not just about how to design and conduct experiments, but also about how to be a responsible and cooperative researcher. I also thank Mario Alfonso Arenas Garcia, Daniel Modafferi, and Zahra Abdali for their editorial help during the preparation of this thesis and the manuscript.

I have to say that starting my Master's study during the pandemic was not easy, and I could have struggled even more without the support from the members of the Dorval Lab. Our lab is simply wonderful. I appreciate that we always help each other troubleshoot experiments, care about each other's feelings, and support each other unconditionally. I also love our shared passion for going on food adventures and cooking for each other.

Daniel, I am so grateful to share an office with you. Thank you for always providing the most detailed and greatest explanations for science, research, Montreal & Quebec, squash, French, and Italian recipes. I deeply appreciate that you keep an open mind for different cultures and listen to my positive and negative thoughts.

Dalia, you are the first lab member I met and have shared the most knowledge with me. I admire your enthusiasm for research and innovation, and enjoy the experiments surrounded by your jokes and singing. Thank you for sharing a significant portion of the writing for the review article.

Zahra, you are a wonderful mentor and lab manager. Thank you for taking on so many responsibilities when we needed you. I always admire your multi-tasking skills and excellent experiment techniques.

Mario, thank you for being a reliable friend. I appreciate our chats on late nights and your memes. You have helped me so much when I did not know to whom I could speak about my confusion. I look forward to the time when your hard work pays off.

I would like to extend my gratitude to everyone I have interacted with during my study. Thank you: Amy for taking classes and doing the group assignments with me; Catrina for answering my questions about job application and thesis preparation; Slah for the practice conversations in French; Ariel for your bakery; Kingsley for the Cantonese learning lunches and excellent food suggestions; Simon for your help with lab tasks; Juliana for relating to my perfectionism and anxiety.

I am grateful for the funding from McGill for my Master's study and from Mitacs for the project. I am also thankful for the equipment and the assistance from FEMR.

I want to thank my parents for their love and continuous support during my studies in Canada. There is nothing I want more now than reuniting with you.

Finally, I would like to say thank you to my closest family in Canada, my partner, Wenjie, and my furry friend, Tintin. Thank you for accompanying me through the long nights, always believing in me, and accepting my imperfections.

Contribution of Authors

This thesis is presented following the "Guidelines for Thesis Preparation" of McGill University as a manuscript-based thesis for an M.Sc. (Chemical Engineering) candidate. The third chapter of this thesis is a manuscript authored by the M.Sc. candidate in collaboration with co-authors.

The first author, Anqi (Angie) Cai, designed the protocols to fabricate and repair the biofilm-textile composites, performed the mechanical analysis, processed the data, collected the optical microscopic images and some of the scanning electron microscopic images, fabricated the prototypes, and wrote the manuscript.

Zahra Abdali is the second author of the manuscript. She contributed significantly to the conceptualization of the project, performed the wettability and breathability tests, analyzed the results, prepared some of the scanning electron microscopic images, and provided constructive feedback while revising the work.

Dalia Jane Saldanha is listed as the third author of the manuscript due to her contribution to conceptualizing the project and her help with sample preparation and experimental work.

Masoud Aminzare appears as the fourth author to reflect his work of preparing the scanning microscopic images in Figure 4.

The corresponding author, Prof. Noémie-Manuelle Dorval Courchesne, supervised and advised the work.

All authors conceived the project and are co-inventors on a patent application.

Manuscript Details:

(Submitted to Scientific Reports)

Endowing textiles with self-repairing ability through the fabrication of composites with a bacterial biofilm

*Anqi Cai, Zahra Abdali, Dalia Jane Saldanha, Masoud Aminzare, Noémie-Manuelle Dorval Courchesne**

Department of Chemical Engineering, McGill University, 3610 University Street,

Montreal, QC, Canada, H3A 0C5

E-mail: noemie.dorvalcourchesne@mcgill.ca

Keywords: Self-repairing textiles, Biofilm, Curli fibers, Textile composites

Chapter 1. Introduction

High-performance textiles are textiles with enhanced or novel functional properties to withstand various conditions for usage in everyday clothing, protective apparel, medical textiles, and industrial technical textiles[1-3]. Compared to using high-cost fibers with inherent advanced properties, fabricating textile composites is deemed a low-cost and simple solution to endow commercial textiles with high performance[4]. By modifying textile surface with functional agents such as polymers, nanomaterials, and biomolecules, conventional textiles like cotton have been engineered to display high performance in advanced applications like self-repairing[5-7], self-cleaning[8-10], antimicrobial activity[11-13], and thermal management[14-16]. Among the functional agents that have been introduced into textile composites, biologically-derived materials, such as proteins, have attracted interest because they are biodegradable, renewable, and biocompatible, which is in line with the efforts toward green and sustainable production[17]. Synthetic biology has expanded the toolbox to replicate and modify the proteins in nature, enabling the scalable production of protein-based materials with desired properties, including self-healing, environmental responsiveness, and remarkable mechanical strength[18]. Incorporating these biologically-derived materials with properties tailored to advanced functionalities into conventional textiles will provide new prospects for the sustainable and economical production of high-performance textiles.

Engineered living materials (ELMs), containing living cells and a multitude of components formed by the cells, have attracted increasing research interests in recent years[19]. Compared to proteins or other biopolymers, ELMs harness the biological functions of the living component. They can use energy and nutrients from their environment to synthesize biopolymers, autonomously self-assemble into complex structures, regenerate, and respond to the environment over the lifetime of the living component[19,20]. One of the well-studied ELM systems is the biofilm of *Escherichia coli*

(*E. coli*), which consists of a matrix of extracellular polymeric substances and bacterial cells embedded in the matrix[21]. The formation of biofilms enhances bacterial cell-to-cell interaction, promotes surface colonization, and protects the bacteria in harsh environments[22]. Through genetically programming the biomolecules produced by bacteria and secreted in the biofilm's extracellular matrix, biofilm serves as a low-cost and efficient platform to engineer and produce biomaterials with living properties[23].

The primary proteinaceous structural component in *E. coli* biofilms is amyloid curli fibers. Owing to their ordered β-sheet rich structure, amyloid curli fibers are known for their mechanical strength and resistance to protease and harsh solvents[24-27]. They have been genetically engineered to exhibit various properties and perform functions both as purified protein-based materials[28-31] and in biofilms[32-36].

Although biofilms adhere to textiles due to textiles' roughened surface and porous structure[37], few studies have investigated the integration of engineered curli biofilms into textiles for improving textiles' functional performance. By exploiting the mechanical stability and tunability of curli fibers as well as the living properties of biofilms, curli-expressing biofilms have the potential to imbue conventional textiles with enhanced mechanical properties, self-repairing abilities, and various functionalities for wearable, smart textile applications.

1.1 Thesis Objectives and Summary

Objectives

In this thesis, we aimed to introduce ELMs into conventional knitted textiles through green processes to fabricate composites with improved performance and functionalities. As a proof of concept, we sought to incorporate engineered curli biofilms from *E. coli* into cotton textiles to

endow the textiles with enhanced mechanical properties and self-repairing ability. The first objective we hoped to achieve was fabricating biofilm-textile composites with tunable biofilm density using simple procedures. Then, we sought to assess the physical and mechanical properties of the composites and how the different preparation methods would affect the properties. The final objective of this thesis was to explore the self-repairing ability of the composites endowed by introducing the biofilms and the strength of the repaired material.

Hypothesis

We hypothesized that introducing *E. coli* curli biofilms would endow the textiles with water-inducible self-repairing ability, while retaining and even enhancing the physical and mechanical properties of textiles relevant to wearable applications.

Summary

We integrated *E. coli* biofilms containing expressed curli fibers into knitted cotton textiles through three simple, fast, and scalable techniques: adsorption, doctor blading, and vacuum filtration. Upon viewing the composites with optical and scanning electron microscopy and measuring the integration densities, we noticed that these methods led to the formation of biofilm coatings or layers with different morphologies and allowed for tuning biofilm density per textile surface area. We evaluated the mechanical characteristics of the composites using tensile tests and the water vapor transmission rate through the material, confirming that the composites remained strong and breathable after the biofilm integration. It is noteworthy that biofilm adsorption enhanced the textile's elastic modulus by an average of 120%, while composites containing vacuum-filtered biofilm were ~140% more extensible at break than the original textiles. To demonstrate biofilm-induced repair, we rehydrated and joined the ends of broken composite pieces, and then dried the

pieces under ambient conditions. By characterizing the mechanical response of the patched and the welded composites using single lap shear tests and tensile tests, respectively, we showed that the composites made with all three methods effectively repaired centimeter-scale defects.

Chapter 2. Literature Review

2.1 High-performance Textile Composites

Textiles are key components of our daily life. Evidence shows that textile use in clothing may date back about 50,000 – 100,000 years[38]. Nowadays, textiles are associated with our aesthetic expression, cultural identification, and practical demands. They are found in diverse applications, including fashion and functional apparel, textile art, and technical textiles[39]. Innovations in textiles have been inspired to create sustainable and durable textile products that provide consumers with improved comfort and protection, functional performance, and desirable aesthetic qualities. The demand and the market size for such technology-rich high-performance textiles are expected to be fast-growing[4].

In contrast to using complex, high-cost fibers with inherent advanced properties, modifying conventional textiles and fibers by incorporating external functional materials is a more cost-effective approach[4]. A variety of advanced materials have been employed to prepare high-performance textile composites, with a significant portion being organic and inorganic nanomaterials because of their stability, processability, light weight, and specialized functionalities[40,41]. To date, textile composites have been created in research studies for a broad range of applications to meet four major demands: comfort, ease of care, protection, and smartness. As one of the top priorities in apparel design, comfort has been enhanced by textile hybrids with thermal management abilities[14-16]. Easy-care textile composites capable of self-cleaning[8-10] and self-repairing[5-7] are desired to prolong textiles' lifetime and reduce textile waste. The protection functions of textile composites against various hazards such as fire[42,43], electromagnetic radiation[44], and bacterial infections[11-13] have enabled the fabrication of protective apparel and

technical textiles. Last but not least, smart textile composites with sensing[30], conductive[45,46], and energy harvesting[47] properties have been explored for making wearable sensors and electronics.

2.2 Self-repairing Textiles

At every stage of their lives, textile products have a substantial ecological footprint, impacting the environment and climate change[48,49]. As a crucial sector in the economy, textile production requires the intensive use of natural resources (water, land, energy), petroleum-based synthetic polymers, and hazardous chemical additives. It also involves significant greenhouse gas emissions[49]. Driven by the growth of the fast fashion industry, textile consumption keeps skyrocketing, leading to tremendous textile waste[50]. According to estimates, 92 million tons of textile waste are generated annually on a global scale; by 2030, this number is expected to increase by 45%[51]. These waste textiles are directly disposed of in the environment as solid waste, deposited in landfills, or incinerated, intensifying environmental pollution and threatening public health[50,52].

To reduce the net greenhouse gas emissions, the European Commission has recently adopted a set of proposals as part of the European Green Deal and Circular Economy Action Plan, one of which is the *EU Strategy for Sustainable and Circular Textiles*[53]. The strategy highlighted the mandatory eco-design requirements in the textile industry[53]. Textiles should be durable, reusable, repairable, and recyclable; they should be made with non-hazardous materials in a green, sustainable way[48,53] (Figure 1).

Indeed, as 40% of the reasons for consumers discarding clothes may be attributed to the functional defects of the clothes, repairing clothes appears to be effective in reducing textile waste[49]. However, many consumers do not have the skills or willingness to do so. An innovative solution to this problem is to develop textiles that can repair mechanical defects on their own and restore

their morphological, mechanical, and functional features. These textiles are defined as "self-repairing" textiles. [54]

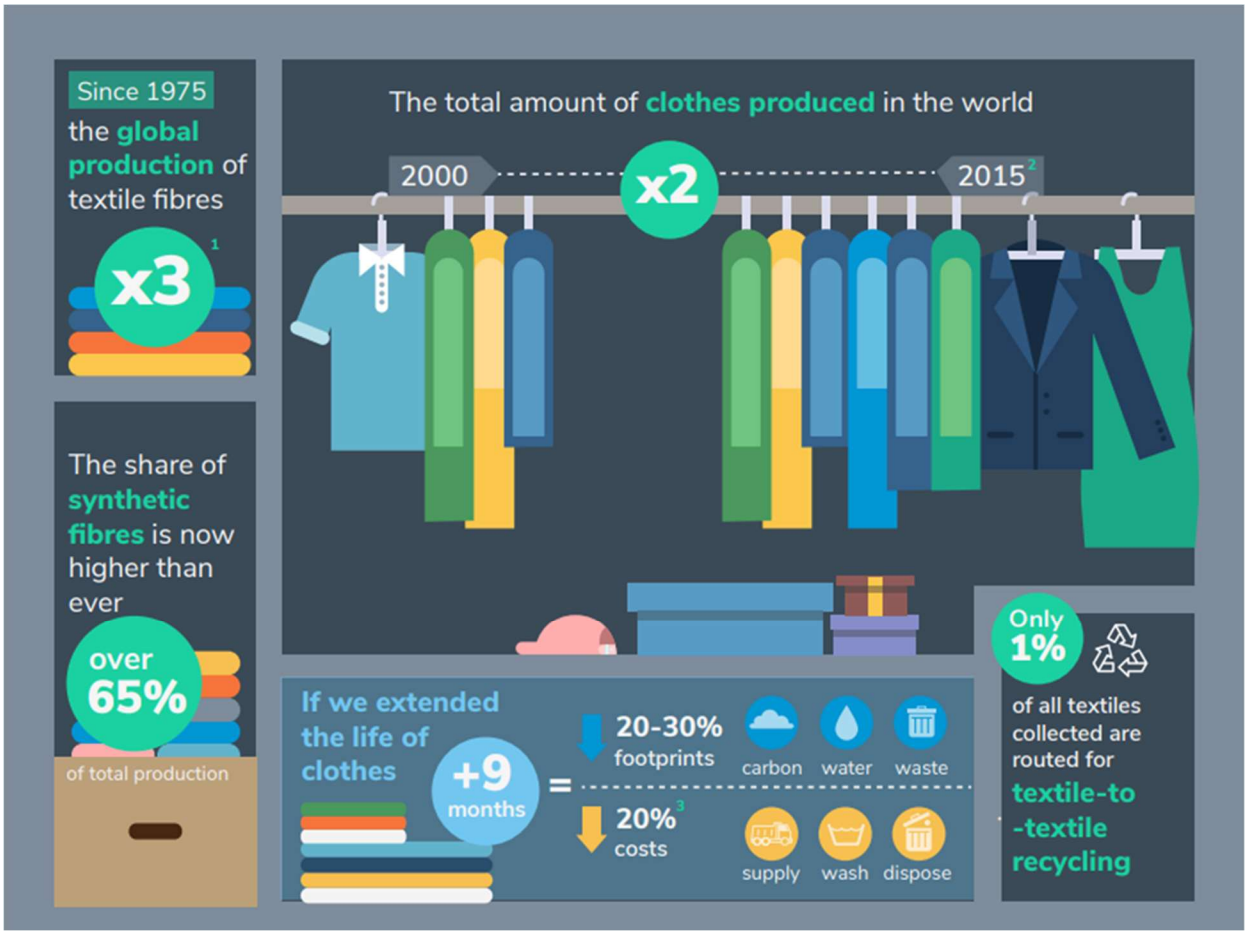

Figure 1. The increased environmental footprint of textile production and the urgent need to extend textiles' lifespan through eco-design[48].

Many reported self-repairing textiles are composites made by incorporating external repair agents into regular textiles. Activated by external stimuli or acting autonomously, these repair agents facilitate the repair of defects that have sizes ranging from nanometer- to centimeter-scale and are generated physically (e.g., cut, abrasion, scratch) or chemically (e.g., UV radiation, plasma treatment) [54]. After the self-repair, specific properties or functions of the textile composites are

recovered, some examples of which are wettability[55,56], barrier properties[57], mechanical properties[57], and visual morphology[58] (Figure 2). These recovered properties can be quantitatively measured and compared with the values of the undamaged materials to determine the efficiency of repair.

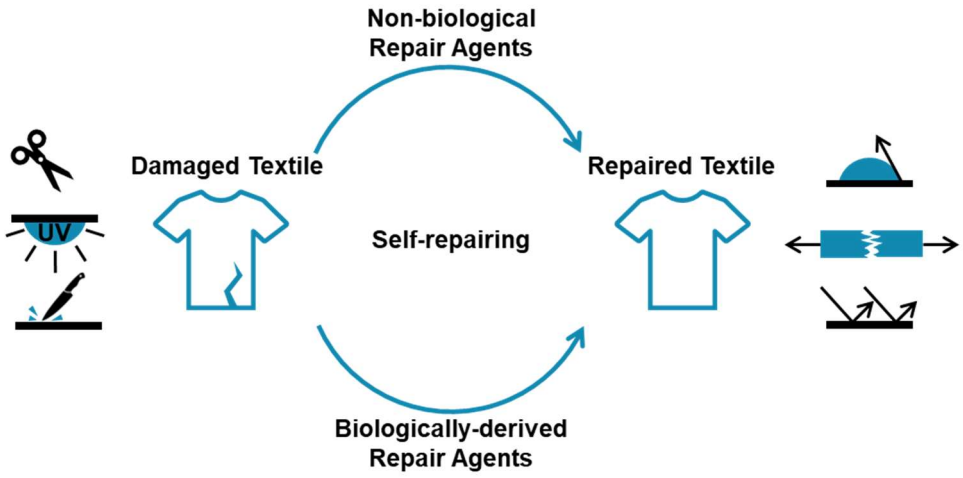

Figure 2. A scheme of self-repairing textiles. By incorporating repair agents, damaged textiles can restore their properties such as wettability, mechanical strength, and barrier properties.

2.2.1 Non-biological Repair Agents

Various repair agents and strategies to integrate the agents into textiles have been developed for the fabrication of self-repairing textiles. One of the earliest reports on self-repairing textiles and one of the most researched is the use of fluorine-based molecules and polymers as textile coatings[6,59]. In 2011, Wang *et al.* dip-coated woven polyester fabrics with an ethanol solution of fluorinated-decyl polyhedral oligomeric silsesquioxane (FD-POSS) and fluorinated alkyl silane (FAS) to make textiles that repaired damages caused by plasma treatment, acid and base solutions, and laundry abrasion[5]. The self-repair was mediated by the self-healing of the FD-POSS/FAS coating and demonstrated through the maintenance of superhydrophobicity and

superoleophobicity after multiple cycles of damage – heat treatment[5]. In contrast, the uncoated textile after the same treatment showed a contact angle of 0°, becoming hydrophilic[5]. The authors proposed that the healing of the coating was due to the molecular movement and reorientation of FD-POSS at an elevated temperature (135°C) which lowered the surface free energy[5]. This super-liquid-repellent coating could be applied to make protective clothing[5]. Since this work was published, many self-repair strategies based on FD-POSS and/or FAS and targeting the recovery of wettability emerged. In addition to FD-POSS and FAS, the group of researchers has also introduced fluoroalkyl surface-modified silica nanoparticles (FS-NPs) to improve the repellency against low surface tension liquids[60] and poly(3,4-ethylenedioxythiophene) (PEDOT) (to enhance the electrical conductivity[61]. Other modifications to the coating formula that used materials such as poly(vinylidene fluoride-hexafluoropropylene) (PVDF-HFP)/FAS/silica nanoparticles[56], vinyl-terminated polydimethylsiloxane (V-PDMS)/tri-functionality vinyl perfluoro decanol (TV-PFOD)/octavinyl-POSS (OV-POSS) [62], palygorskite (PAL)/1H,1H,2H,2H-perfluorodecyltriethoxysilane (PFDTES)/tetraethoxysilane (TEOS) [63] are all based on a similar self-healing mechanism – the molecular migration of fluorinated chains lowering the surface energy.

Following the fluorine-based compounds, other non-biological materials, including silane-based molecules (e.g., polydimethylsiloxane (PDMS) [64], dodecyltrimethoxysilane[65]), graft polymers (e.g., poly[(methyl methacrylate)-*b*-(trifluoroethyl methacrylate)] [66]), nanomaterials (e.g., MnO_2[67]), have been reported as repair agents in textiles. Although these repair agents appear to be effective in restoring certain properties of textiles, a majority of them functioned on limited size scales (e.g., individual fiber level to mm-scale), as noticed by *Ramesh et al.* in their review[54]. In addition, some chemistries involved in the self-repair process are complex and even toxic. For

example, many fluorine-based compounds have raised environmental and health concerns due to bioaccumulation and might lead to several diseases[68]. Furthermore, Zhou *et al.* pointed out that most self-repairing coatings developed involved large amounts of organic solvents, such as ethanol[5,69], acetone[69,70], and dimethylformamide[70], resulting in pollution and safety concerns in production[59]. These concerns hinder the production of these self-repairing textiles at industrial scales and limit their application in repairing common mechanical defects on clothes in practical use. Therefore, fluorine-free, solvent-free strategies for making self-repair textiles need to be explored.

2.2.2 Biologically-derived Repair Agents

Biologically-derived materials, such as proteins, have been extensively exploited for wearable applications, because of their biocompatibility, biodegradability, and renewable resources[71]. Protein fibers from nature, such as silk and wool, have a long history of use in textile fabrication[72]. Many protein-based materials used for wearables belong to the category of structural proteins[71]. Produced by a wide variety of organisms, these proteins self-assemble into hierarchical structures that contribute to the organisms' mechanical integrity[73].

One example of structural proteins is squid ring teeth (SRT), lined on the tentacles of decapodiform cephalopods (squid and cuttlefish) [74]. In nature, these animals use their tough teeth to firmly grasp the prey. Exhibiting a high Young's modulus of 4.5 – 7.5 GPa in the dry form and 1.75 – 2.75 GPa when hydrated, SRT show remarkable mechanical properties comparable with those of some strong synthetic polymers[75]. The mechanical properties of SRT are stemmed from their semicrystalline structure, formed by repetitive and alternating rigid β-sheet forming (crystalline) domains stabilized by hydrogen bonding and long, flexible amorphous domains[76]. The crystalline domains provide physical cross-links, while the amorphous domains are stretchable strands that

entangle, leading to SRT'S network morphology and mechanical properties[76]. Compared to harvesting naturally occurring SRT from squids and cuttlefish that are captured for human consumption, the recombinant production of SRT in commercial host organisms is more desirable due to the higher yield, lower cost, and room for modifications[77].

A recombinant SRT protein has been made into films that self-healed after being cut in half and pressed in warm water at 45°C, which was above the protein's glass transition temperature[78]. Their self-healing capability was attributed to the water's plasticizing effect in the amorphous domains and the reinforcement of self-assembled crystalline domains[78]. Inspired by SRT's self-healing capability, Gaddes *et al.* have dip-coated wool, cotton, and linen textiles with purified recombinant SRT proteins. They then built layer-by-layer films on the modified textiles with SRT and polystyrenesulfonate (PSS) to encapsulate urease enzyme[6]. They showed that these coated textiles had improved mechanical strength and could self-repair damages in the millimeter to centimeter range by patching after they were immersed in 70°C water and compressed together using PDMS molds[6]. After the repair, the enzymatic activity of the encapsulated urease was preserved[6]. The authors envisioned that such coating materials could introduce more complex protective functions to textiles[6]. This work is one of the very few attempts to date to employ biologically-derived materials as a repair agent in textiles, and one of the most effective repair mechanisms based on the size scale of repair.

Although success has been reported for the biomimetic engineering and production of natural structural proteins, including SRT, scaling up the production can be difficult[79]. First, these proteins consist of repetitive amino acid sequences[80], which require time-consuming and expensive genetic recombinant techniques[81]. Also, purifying these recombinant proteins usually requires multi-step, costly procedures involving cell lysis, ultracentrifugation, and chromatography[79]. Efforts have

been made to engineer *Caulobacter crescentus* and use its Type I secretion systems to express and extracellularly secrete suckerin-19 (a protein found in SRT), which could have the potential to simplify the subsequent protein purification process[82]. However, the secretion failed because the protein contained ordered β-sheet structure[82]. Therefore, when employing recombinant protein-based repair agents on textiles in practical use, producing sufficient quantities of the agents to repair macro-sized textile defects can be challenging.

2.3 Bacterial Biofilm

Previous studies on synthetic biology and biological pathways have allowed cells to be used as factories to produce substances with commercial values. Recently, efforts have been made to use living systems containing cells that construct or assemble large structures and modulate the material's properties as a novel platform to engineer advanced materials. These living systems are named "engineered living materials" (ELMs) [19]. Because they are living, ELMs can self-regenerate, self-organize, and respond to the environment[83]. They can also be genetically or chemically modified and patterned to exhibit desired physiochemical and mechanical features[19]. Plus, multifunctional hybrid systems can be designed by interfacing ELMs with inorganic materials and combining the abilities owned by the two types of materials.

One of the most studied ELM models is bacterial biofilms, formed by bacterial cells and the substances secreted and assembled by the cells in their extracellular matrices[84]. Their structural stability, pathogenicity, and ability to colonize various surfaces and protect cells from the surrounding environment lead to their negative reputation in food, textiles, marine, construction, and many other industries[22,85]. For instance, biofilms formed by skin bacteria introduced to clothes during sweating cause sweat malodor, discoloring, and decreased textile quality[86]. Biofilms on clothes can be difficult to remove by conventional laundry, and the strong adhesion is attributed

to textiles' roughened surface, large pore volumes, and hydrophobic and hygroscopic properties[37,86]. Thus, combating textile biofilms and designing anti-biofouling clothing have long been of interest.

Some studies envisioned instead the colonization of biofilms on textiles as a tool for engineering environment-responsive wearables. By genetically engineering the CsgA subunit of the structural protein, curli fibers, in *Enterobacteria* biofilms with a multichromatic control system consisting of promotors P_{T3}, P_{CGG}, and P_{K1F}, biofilms were generated and patterned in response to different colors of light[36]. The blue light-induced biofilms formed on various surfaces, including glass, mica, plastics, and woven cotton textiles[36]. On textiles, the bacteria expressed curli fibers under blue light, which increased the biofilm attachment to the textiles[36]. The adhered bacteria remained alive after mechanical washing and responded to a second light source to produce green fluorescence with the insertion of the gene encoding green fluorescent protein (GFP) [36]. This study demonstrated the programmability of biofilm as a responsive living material and the potential to produce composite materials with inorganic scaffolds, like textiles. Another study that exploited biofilms' ability to sense and respond to create textile hybrids was done by Raab *et al*. They allowed the biofilm of *Bacillus subtilis* to repair fabrics in response to mechanical tears by expressing a silk protein programmed to self-assemble into fibers after secretion[87]. Their work highlighted the biofilm's ability to regenerate biologically when integrated into hybrid systems. Wang *et al.* exploited the hygroscopic behavior of microbial cells. They modified latex sheets to engineer wearables capable of modulating ventilation by microprinting several types of biofilm-producing cells onto the latex substrate[88]. The created hybrid films bent at dry conditions (relative humidity 15%) due to cell dehydration, and flattened at humid conditions (relative humidity 95%) due to the increased cell volume after water was regained[88]. The authors also introduced biofluorescence

into the *E. coli* cells of the hybrid films by genetically engineering the cells to express GFP and found that the fluorescence intensity of GFP varied with environment humidity[88]. Based on their findings, they designed a running suit and a shoe as prototypes with the fluorescent, humidity-responsive ventilating fabrics and demonstrated that this design enabled skin sweat removal and temperature control[88].

2.3.1 Components and Functions of *E. coli* Biofilm

E. coli is a Gram-negative, rod-shaped bacterium found in vertebrates' gastrointestinal tract, where *E. coli* is present in the form of biofilm[89,90]. In biofilms, *E. coli* cells are embedded in matrices formed by extracellular polymeric substances (EPS), including exopolysaccharides, nucleic acids, proteins, and lipids (Figure 3). The table below summarizes several major components of *E. coli* biofilm and their functions.

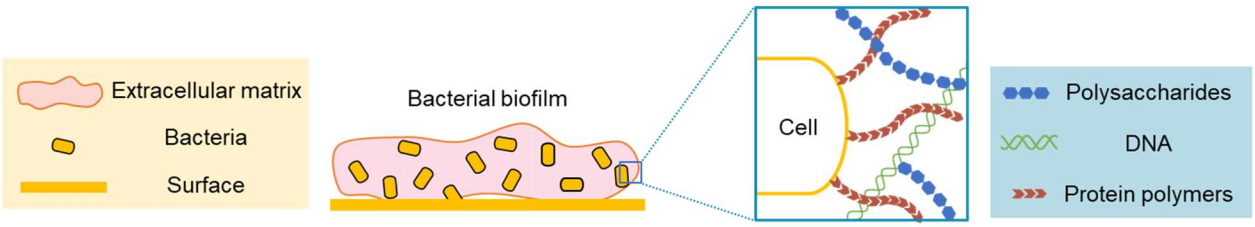

Figure 3. A scheme of bacterial biofilm whose extracellular matrix mainly consists of polysaccharides, proteins, and DNA.

Table 1 A summary of the major extracellular matrix components in E. coli biofilm and their functions

Name	Description	Function	Ref.
Type 1 fimbriae (pili)	Filamentous proteinaceous adhesins	• Involved in irreversible surface adhesion at the early stage of biofilm formation	91,92

Curli fibers	Amyloid proteinaceous fibers with a β-sheet-rich structure	• Improving the stability and strength of extracellular matrices • Involved in the adhesion of biofilms to human cells and abiotic surfaces • Facilitating cell-surface interaction and cell-cell interaction	[91,93]
Cellulose	A homopolysaccharide consisting of β (1→4) linked D-glucose units	• Enhancing biofilms' cohesion, elasticity, and stability • Improving biofilms' resistance to environmental stress	[94,95]
Lipopolysaccharides (Endotoxin)	Glycolipidic polymer toxins	• Affected biofilm formation by interacting with adhesion factors exposed on cell surface	[91]

2.3.2 Curli Fibers in Biofilm

Despite the fact that polysaccharides constitute the bulk of *E. coli* biofilm EPS mass, programming them can be challenging because of the complex pathway engineering required[23]. In contrast, proteins are considered highly programmable, as their structures and functions can be modified by altering their amino acid sequence[23]. One common way to engineer *E. coli* biofilm is through programming amyloid curli fibers, the primary structural proteinaceous component in the extracellular matrix of *E. coli*.

First discovered in the 1980s on *E. coli* strains, curli fibers are protein nanofibers with a diameter of approximately 4–7 nm found to form tangled networks and embed bacterial cells in the extracellular matrix of *Enterobacteriaceae*[32,96] (Figure 4a). They play a pivotal role in bacterial surface adhesion, cell-cell interaction, biofilm formation and integrity, and pathogenesis[96]. They have been shown to adhere strongly to various abiotic surfaces, owing to the reorientation of the

flexible regions, side-chain interactions, and charged, polar amino acid residues[97]. Encoded by *csgBAC* and *csgDEFG* operons, curli fibers are self-assembled from the major structural subunit CsgA, a 13-kDa protein secreted from the cells and nucleated and anchored to the cell surface by the minor subunit, CsgB[98,99]. The *csgDEFG* operon encodes four accessory proteins that play different but crucial roles in the nucleation and extracellular secretion of curli[96,100]. Curli fibers have the characteristic cross-β sheet structure of amyloids stabilized by hydrogen bonding and hydrophobic interactions and composed of repeating strand-turn motifs[101,102] (Figure 4b). Because of such an ordered structure, amyloids have exceptional mechanical strength, stability, and resistance to harsh environments. Exhibiting a Young's modulus of 3-20 GPa, amyloids are deemed one of the stiffest known biopolymers[25]. They also resist enzyme digestion and denaturation by heat and harsh solvents like sodium dodecyl sulfate and urea[24,27,103].

Engineered curli biofilms and curli-based proteins have been produced by transforming commercial plasmids that contain genes encoding curli fibers into engineered *E. coli* strains, such as PQN4[32]. PQN4 is derived from LSR10 (MC4100, *ΔcsgA*, λ(DE3), Cam^R), whose entire native curli operon has been removed[32]. This strain is suitable for studying curli biogenesis as it does not produce many other extracellular substances in *E. coli* biofilm, such as cellulose, other fimbrae, or flagella[96,104,105]. Taking advantage of curli fibers' aggregation behavior, curli biofilm can be collected directly from the bacterial culture by centrifugation or vacuum filtration[106]. The culture can also be filtered under vacuum through a microporous filter membrane and treated with solvents to purify curli fibers and curli-derived proteins[107] (Figure 4c). The simple, fast, low-cost production of curli fibers and curli biofilms has shown promise for the green, scalable fabrication of mechanically robust, bulk protein-based biomaterials and ELMs.

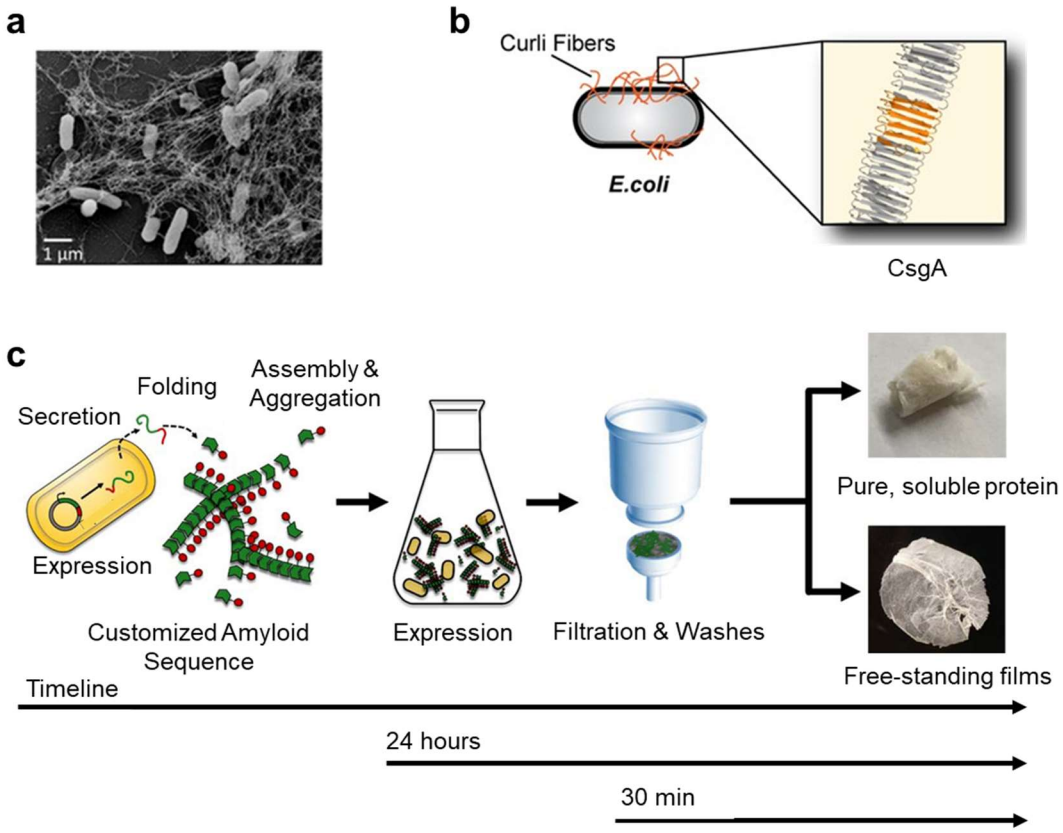

Figure 4. Curli fibers in E. coli biofilm and their production process. (a) An SEM image of curli fibers expressed in E. coli PQN4 strain forming biofilms. This figure was adapted from Dorval Courchesne et al. [107]*. (b) A scheme of curli fibers formed by the self-assembly of CsgA and adopting a cross-β sheet structure. This figure was adapted from Duraj-Thatte et al.* [108]*. (c) An overview of the workflow of fabricating macroscopic curli fibers and curli-derived materials, which included genetic engineering, transformation, protein expression, and vacuum filtration. This figure was adapted from Dorval Courchesne et al.* [107]*.*

2.3.3 Self-Healing Properties of Curli Fibers

Several studies have highlighted an interesting self-healing behavior of curli fibers. Duraj-Thatte *et al.* fabricated aquaplastic sheets using aquagels of curli biofilm or curli fibers and demonstrated their ability to heal scratches and cuts after being rehydrated with water[106]. These sheets can be

welded into 3D structures using water as a "glue", and the welded aquaplastic displayed a Young's modulus of 605 ± 206 MPa[106] (Figure 5a). Our group has investigated this self-healing behavior in curli fiber-PEDOT:PSS composite films[109]. The introduction of curli fibers allowed the biocomposite to self-heal cuts and restore its electrical conductivity after water was added[109] (Figure 5b, 5c).

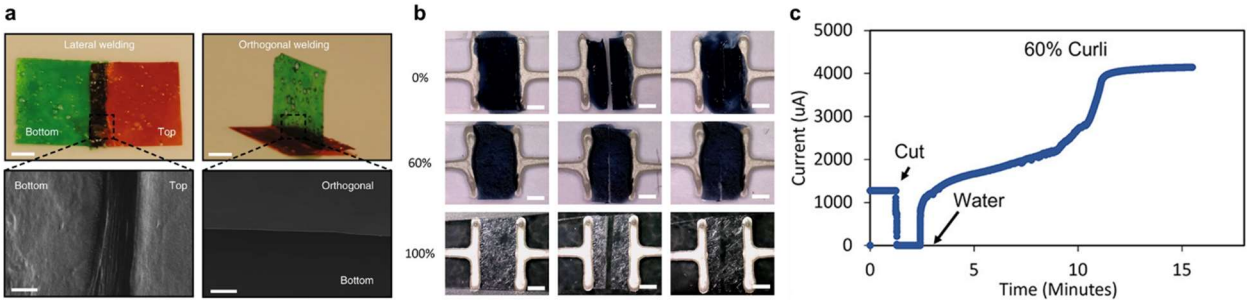

Figure 5. The self-healing behavior of curli biofilm aquaplastic and curli fiber-PEDOT:PSS composites. (a) Optical and field-emission scanning electron microscopy (FESEM) images showing curli biofilm aquaplastic welded laterally and orthogonally after water was added. The scale bars are 5 mm (top row optical images) and 20 µm (bottom row FESEM images). This figure was adapted from Duraj-Thatte et al. [106]. (b) Optical microscope images of PEDOT:PSS thin films containing 0, 60, and 100% (w/w) curli fibers cast between electrodes, cut in half, and healed by rehydration. The scale bars are 500 µm. This figure was adapted from Huyer et al. [109]. (c) Current change over time during the self-healing process of curli-PEDOT:PSS films at an applied voltage of −0.5 V. This figure was adapted from Huyer et al. [109].

The principle behind curli fibers' ability to self-heal mechanical damages has not been fully elucidated. One possible explanation is that after the addition of water, curli fibers swell and gelate. The hydrogelation process has been seen in many amyloids[110]. During this process, curli first aggregates and self-assembles into fibrils, which is driven by multiple intra- and intermolecular

interactions[26,111,112]. This step was followed by fibril entanglement and water-filled 3D supramolecular networks formed through side-chain mediated non-covalent interactions [110,113]. When dry curli fibers are rehydrated, these molecular interactions are restored, and the inter-fibrillar entanglement is increased, leading to the reformation of the fibrillar network and the healing of the bulk material.

2.3.4 Novel Functional Properties Engineered into Curli Fibers

By capitalizing on the facile engineering and production of curli fibers, many innovative features have been engineered into curli fibers to create novel biomaterials. Our group fused a pH-responsive fluorescent protein, pHuji, to the C-terminus of CsgA and vacuum-filtered the engineered curli fibers through a non-woven acrylic textile to create a wearable sweat pH sensor[30]. The resulting curli-textile composite displayed reversible sensing ability over days and remained stable in several solvents[30]. Curli fibers have also been modified on their genetic level by strategies such as replacing the internal repeats in *csgA* gene with a hydroxyapatite (HAP)-binding peptide to template minerals[31], fusing CsgA with mussel foot proteins (Mfps) of *Mytilus galloprovincialis* to make an underwater adhesive[28], and introducing mutations to CsgA to create aromatic mutants with increased conductivity[29].

For this thesis, the strategies to engineer bacterial biofilms into functional ELMs through the curli system are more of interest. For example, Nguyen *et al.* genetically introduced peptide domains to the C-terminus of CsgA. They enabled the *E. coli* biofilms expressing the CsgA fusions to template silver nanoparticles, demonstrate strong adhesion to stainless steel, and immobilize proteins covalently[32]. *Kalyoncu et al.* used a different strategy to create conductive *E. coli* biofilms by expressing CsgA-derived peptide with conductive peptide motifs inserted[33]. Duraj-Thatte *et al.* turned *E. coli* biofilms into cell-laden hydrogels with therapeutic applications in the gut by

encoding mucoadhesive CsgA fusion proteins with trefoil factors and vacuum filtering the cultures producing the modified biofilms[34]. Built upon the CsgA-Mfp fusion protein and the blue light control system reported previously, a work by Wang *et al.* presented living composite materials based on HAP mineralization and biofilms that expressed engineered CsgA proteins under blue light control[35].

2.3.5 Promises for Combining Curli Biofilm and Textiles

Textiles have been studied and employed as a lightweight, low-cost, safe, and flexible scaffolding material for smart devices and wearables[114]. Their mechanical properties that are comparable to those of human skin allow them to conform to body movements and accommodate deformation[115]. Their porous structure enables water vapor transmission[116] and mass transfer[117] through the material. Through physical adsorption and covalent bonding, proteins can be attached to textiles, making textiles promising carrier materials for a variety of biotechnical applications[117,118].

Curli biofilms are regarded as a desired platform to create mechanically stable, multifunctional ELMs with environment-adaptive properties through green production processes. Curli fibers not only provide biofilms with mechanical integrity, protection in harsh environments, and adhesion to surfaces, but also display various novel functions in biofilms when genetically programmed. The self-assembly behavior of curli allows the protein to be loaded into textile matrices in a fast, scalable, and efficient manner[30]. Evidence has shown that after they were fabricated into composites with other polymers, curli fibers remained functional and improved the materials' overall mechanical performance[109,119]. When integrated into nonwoven textiles, engineered curli fibers endowed the textiles with a pH-sensing ability sustained over a few days, without substantially compromising the textiles' mechanical properties or breathability[30]. Furthermore, living bacterial cells that do not produce extracellular matrix components have been drop-cast and

dried to make stiff, stable, self-regeneratable films[120]. Therefore, combining ELMs derived from curli biofilms with textile scaffolds, has the potential to endow the textiles with improved mechanical performance, self-repairing abilities, and environment-responsiveness.

Chapter 3. Endowing textiles with self-repairing ability through the fabrication of composites with a bacterial biofilm

*Anqi Cai, Zahra Abdali, Dalia Jane Saldanha, Masoud Aminzare, Noémie-Manuelle Dorval Courchesne**

Ms. Anqi Cai, Dr. Zahra Abdali, Ms. Dalia Jane Saldanha, Mr. Masoud Aminzare, and Prof. Noémie-Manuelle Dorval Courchesne

Department of Chemical Engineering, McGill University, 3610 University Street,

Montreal, QC, Canada, H3A 0C5

*E-mail: noemie.dorvalcourchesne@mcgill.ca

Keywords: Self-repairing textiles, Biofilm, Curli fibers, Textile composites

Abstract

To address the increasing environmental footprint of the fast-growing textile industry, self-repairing textile composites have been developed to allow torn or damaged textiles to restore their morphological, mechanical, and functional features. A sustainable way to create these textile composites is to introduce a coating material that is biologically derived, biodegradable, and can be produced through scalable processes. Here, we fabricated self-repairing textile composites by integrating the biofilms of *Escherichia coli* (*E. coli*) bacteria into conventional knitted textiles. The major structural protein component in *E. coli* biofilm is a matrix of curli fibers, which has demonstrated extraordinary abilities to self-assemble into mechanically strong macroscopic structures and self-heal upon contact with water. We demonstrated the integration of biofilm through three simple, fast, and scalable methods: adsorption, doctor blading, and vacuum filtration.

We confirmed that the composites were breathable and mechanically strong after the integration, with improved Young's moduli or elongation at break depending on the fabrication method used. Through patching and welding, we showed that after rehydration, the composites made with all three methods effectively healed centimeter-scale defects. Upon observing that the biofilm strongly attached to the textiles by covering the extruding textile fibers from the self-repair failures, we proposed that the strength of the self-repairs relied on both the biofilm's cohesion and the biofilm-textile adhesion. Considering that curli fibers are genetically-tunable, the fabrication of self-repairing curli-expressing biofilm-textile composites opens new venues for industrially manufacturing affordable, durable, and sustainable functional textiles.

Introduction

The textile industry constitutes an important sector of the global economy. The demand for fast fashion has resulted in increased production of clothing, footwear, and household fabrics, leaving behind an indelible environmental footprint[1]. Specifically, textile production involves substantial use of land, water, and raw materials, part of which are synthetic fibers sourced from fossil fuels. Textile consumption also raises environmental concerns due to improper disposal of unwanted or damaged clothes[2]. To tackle these problems, improving the durability and repairability of clothes is crucial, because functional damages, such as wear and tear, often account for consumers prematurely discarding their clothes[3].

Recently, researchers have proposed some creative solutions to enable conventional textiles to self-repair permanent damages and regain lost morphological and functional characteristics. In particular, they employed self-healing polymers as textile coatings to create textile hybrids that can recover damages in response to environmental changes[4]. Although various physical coatings and chemical surface modification methods have been developed, most self-repair mechanisms

reported only recover superficial, micro-sized damages or damages on individual fibers[4,5]. In addition, the industrial applicability of these self-repair mechanisms remains uncertain due to the complexity of the required chemistries and techniques, the biotoxicity and bioaccumulation of certain coating chemistries[6], and the safety and pollution concerns associated with using organic solvents[7,8].

Modifying conventional textiles with self-healing biological materials presents an alternative solution to repair textiles, because these materials are biocompatible, biodegradable, and have the potential for genetic customization. For example, structural proteins that self-assemble into higher-order structures in nature and exhibit outstanding mechanical strength are usually used for the mechanical improvement of composite materials and devices[9]. Through synthetic biology, structural proteins, such as Squid Ring Teeth proteins and silk proteins, have been produced by bacteria and applied in the fabrication of self-repairing textiles[10,11]. In these textile hybrids, novel functions, including biomolecule incorporation[10] and environment-responsive self-regeneration[11], have also been enabled. However, recombinant protein production and purification at an industrial scale can be costly[12], hampering the practical use of these proteins in textile repair.

Recently, biofilms that are naturally self-produced by bacteria and self-assemble into higher-order structures have been exploited as biomaterials and incorporated into textile composites. Biofilms are co-adhered microbial cells enclosed in extracellular polymer matrices and attached to surfaces[13]. This material has the potential to be industrially produced in inexpensive, scalable, and non-polluting processes, hence complying with green and sustainable production. Textiles' roughened surfaces and large pore volumes facilitate the development and adhesion of biofilm[14], which inspired the construction of biofilm-textile hybrids[13,15,16]. Biofilm formation protects the

biological activities of cells from environmental stresses, rendering the biofilm-textile composites self-regeneratable and environment-adaptable[15,16].

Within the biofilms of enteric bacteria like *Escherichia coli* (*E. coli*), amyloid curli fibers are expressed as the major proteinaceous extracellular structural component and mediate cell-cell and cell-surface interactions[17,18]. The major subunit of curli fibers, CsgA, is secreted outside the cell membrane and nucleated and anchored to the cell wall[19]. By fusing CsgA with non-native peptides on the genetic level, a variety of functional biofilms have been developed for applications such as metal surface adhesion, inorganic nanoparticles templating[20], enzyme immobilization[21], light-inducible biomineralization[22], and therapies for intestine inflammation and gut healing[23,24]. Owing to their ordered, β-sheet-rich structures, amyloids like CsgA exhibit remarkable mechanical properties and stability with Young's moduli ranging from 3 GPa to 20 GPa[25] and resistance to chemical and biological degradation[26]. Of particular interest, thin films made with curli fibers have demonstrated self-healing abilities through healing scratches/cuts and restoring functional features after rehydration with water[27,28]. Upon addition of water, curli fibers swell due to hydrogelation with increasing fibril entanglement and side chain-mediated non-covalent interactions between the fibrils, thus forming polymer networks[29-31]. Also, the recovery of multiple non-covalent interactions and supramolecular hydrogen-bonding networks can drive the self-assembly of curli fibers, promoting structural stabilization and self-healing[32-34].

Inspired by the tunability, mechanical strength, and self-healing ability of curli fibers expressed in biofilms, we integrated curli biofilm into conventional knitted cotton textiles to fabricate self-repairing textile composites. We used three integration methods – adsorption, doctor blading, and vacuum filtration – to cover cotton fibers with biofilm and tuned biofilm density per textile surface area. While retaining breathability, the textile composites have enhanced mechanical properties

depending on the integration method. We showed that the textile composites can effectively repair centimeter-sized cuts by patching and welding in the presence of water, and the strength of repaired composites was determined by the cohesion of biofilm and biofilm-textile adhesion. This work opens the opportunity for the scalable fabrication of sustainable and smart textile composites with novel functionalities and improved lifespan.

Results and Discussion

Fabrication of Biofilm-textile Composites

First, we aimed to fabricate composites with curli-expressing *E. coli* biofilms and cotton/spandex jersey knitted fabrics (Figure S1). To prepare the composites, we used bacterial cultures where amyloid curli fibers were expressed and secreted in the medium (verified with a Congo Red binding assay, Figure S2). We developed three composite fabrication methods that are fast, simple, and scalable to distribute biofilm on the textile surface differently and to endow the composites with different characteristics potentially suitable for a range of applications: method 1) depositing biofilm throughout the textile by incubating the textile in biofilm solutions of various concentrations (adsorption of the biofilm onto the surface of the textile fibers), method 2) applying a uniform biofilm layer with controlled thicknesses onto the textile (doctor blading), and method 3) filtering a concentrated biofilm solution through the porous textile under vacuum (vacuum filtration) (Figure 1a). By altering the quantity of biofilm incorporated, we also aimed to allow for further adjustment of the composites' characteristics.

We sought to compare the surface morphology of the composites made with the three methods. Adsorption resembles the dip coating technique commonly used to introduce compounds from a homogeneous solution with varying concentrations to modify textile surfaces[35]. We immersed the textiles overnight in biofilm solutions of 0.4 g/mL, 1 g/mL, and 2 g/mL (AS-0.4 g/mL, AS-1 g/mL,

AS-2 g/mL) to provide a wet environment for biofilm infiltration into the textile matrix and sufficient time suitable for the irreversible adsorption of biofilm on both surfaces and in the matrix[36]. Biofilm appeared as fragmented pieces of coating on the textile fibers on both sides (Figure 1b, 1c). Using doctor blading, we were able to control and manipulate the thickness of wet biofilm coating with 0.17 mm, 0.51 mm, and 1 mm masks (DB-0.17 mm, DB-0.51 mm, DB-1 mm). Such deposition resulted in a glossy, uniform, and thick layer of biofilm covering the front surface of the textile, with a decreased thickness after drying due to the loss of water in the cells, whereas little biofilm was seen on the back side (Figure 1b, 1c). Finally, we used vacuum filtration (VF) to increase the interaction between the biofilm and the textile substrate[37,38]. We have previously employed this technique in a scalable protocol for purifying engineered curli fibers and integrating curli fusion proteins into non-woven textiles[38,39]. The optical microscope and scanning electron microscopy (SEM) images showed that the biofilm consisting of aggregated curli and cells was entrapped in the porous textile matrix, subsequently preventing more biofilm from passing through the textile. This method created a smooth and dense biofilm packing on the top surface of textiles and left little biofilm observed on the back side (Figure 1b, 1c).

To quantify and compare the amount of biofilm integrated into the dry composites made with each approach, we measured the "integration density" of the biofilm-textile composites, which we defined as the dry weight of biofilm incorporated into per unit area of the composites. The results suggested that the three methods we employed resulted in the integration of 5 – 32 mg of biofilm per square centimeter of textile (Figure 1d). An increasing amount of biofilm was distributed on both sides of the biofilm-adsorbed composites as the textiles were incubated in more concentrated biofilm solutions (Figure S3). Doctor blading the textiles with biofilm pellets using masks of increasing thicknesses created thicker layers of coating only on the front side, leading to the highest

integration density values (Figure S3). We used the clogging of the textile and filter membrane as a sign to end the vacuum filtration process and did not further alter the integration density. The vacuum-filtered composites had an integration density greater than all the composites made with biofilm adsorption, suggesting the vacuum-aided filtration process rapidly accumulated more biofilm on the collecting textiles than the biofilm adsorption process in solutions. The wide range of integration density and the different morphological features have the potential to suit a variety of applications in the textile industry, ranging from functional apparel to technical textiles used in agriculture, construction, and other fields.

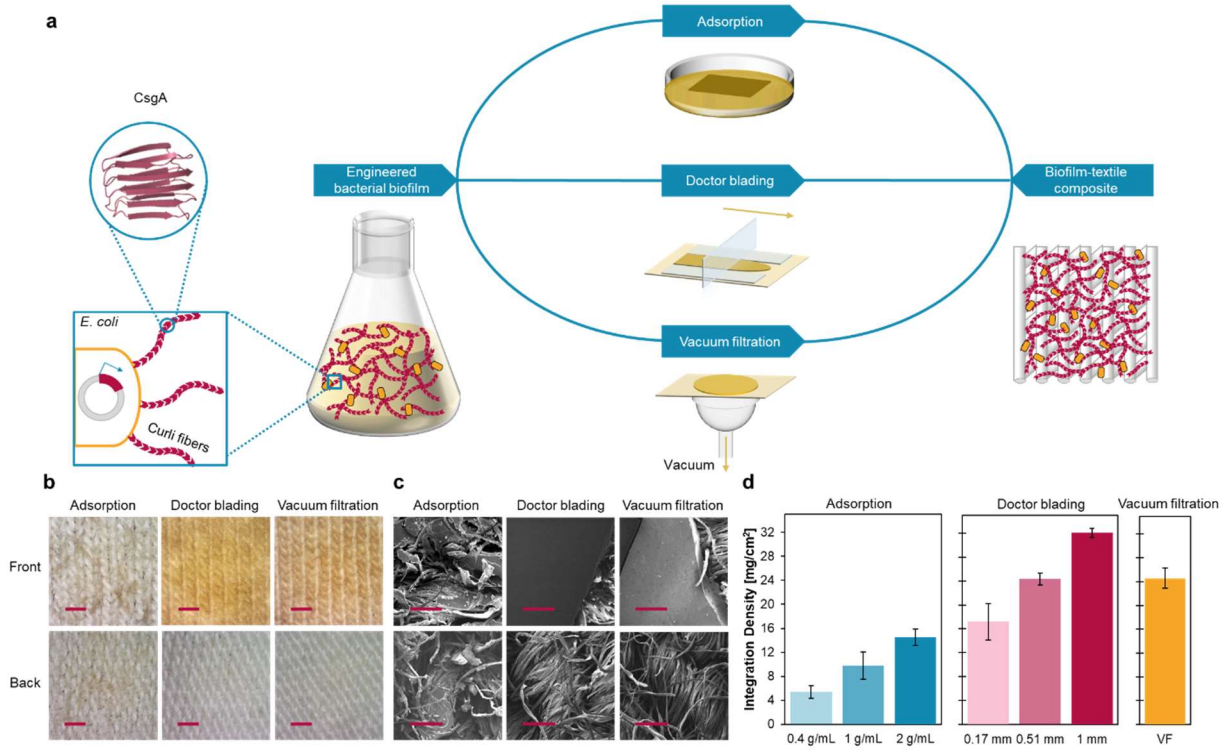

Figure 1. Fabrication of biofilm-textile composites. (a) A scheme of the three methods to integrate biofilm formed with curli fibers, amyloids assembled from CsgA (structure prepared by PyMOL and previously derived computationally[40]), into textiles. (b) Optical microscope images of the front and back sides of the biofilm-textile composites AS-2 g/mL, DB-1 mm, and VF. The scale bars are

1 cm. (c) SEM images of the front and back sides of the samples shown in (b), demonstrating the distribution and coating of biofilm on textile surfaces. The scale bars are 200 µm. (d) Bar plot of the integration density calculated for the composites prepared using the three methods. The bars represent mean values, and the error bars are standard deviations.

Modified or Improved Physical and Mechanical Properties

The motivation to fabricate composites is to combine the advantage of each component[41], so we investigated how biofilm integration modified the textiles' characteristics. Specifically, we examined the biofilm-textile composites for performances of interest for wearable applications: surface wettability, breathability, and mechanical properties. Knowing that the composite morphology and the integration density can be altered by adopting different integration methods, we further assessed if these differences also impacted the composites' physical and mechanical properties.

The moisture management properties of textiles, reflected by the textiles' ability to remove sweat from skin, are essential to provide wearers with a satisfying level of thermo-physiological comfort in wearables[42]. As the first key step in the transportation of liquid sweat, wetting is determined by the textiles' surface characteristics[43]. We studied how adding biofilm coatings using the three methods influenced the textiles' surface properties by comparing the static water contact angles on the front surface of the composites with high densities of integration (AS-2 g/mL, DB-1 mm, VF). Both the doctor-bladed and the vacuum-filtered composites exhibited a decrease in the water contact angle (compared with the plain textile without biofilm integration) (Figure 2a). In these composites, smooth biofilm layers covered the textile surface and reduced the macroscopic surface roughness that was caused by the textiles' knitted structure and the cotton fibers protruding from the surface. The increased wettability of the doctor-bladed and the vacuum-filtered composites

also agrees with the previously reported observation for curli thin films (contact angle of 58.6° ± 1.7°)[44]. We failed to record contact angle measurements with AS-2 g/mL, as the water droplet was absorbed immediately by the composites upon contact. As discussed in the previous section, unlike in the other two methods, the adsorbed biofilm did not completely fill up the pores on the textiles or cover all the textiles' surface features. Adsorption might have modified the textiles' pore size, surface roughness, and hydrophilicity to the extent that the capillary pressure was elevated, and the water droplet quickly filled the surface cavities[45,46].

When sweat is transported in its vapor form by diffusion, adequate vapor transmission through the biofilm-textile composites must be ensured to establish a comfortable microclimate in wearing applications. We measured the water vapor transmission rate (WVTR) for composites with the highest integration densities prepared by each of the three methods (AS-2 g/mL, DB-1 mm, and VF), as we expected denser biofilm coating would hinder the transmission rate more than low-density coatings. Despite the reduced porosity, increased thickness, and the different moisture absorption capability of biofilm, we did not observe a statistically significant difference between the WVTR of each composite and that of the plain textile[47] (Figure 2b). Given that the WVTR of normal skin is 150-450 g m^{-2} day^{-1}, the fabricated biofilm-textile composites remained breathable[48].

Being mechanically strong is crucial for clothing fabrics to withstand daily wear and have a long lifetime, so we conducted tensile tests on the textiles before and after biofilm integration to determine the Young's moduli and the elongation at break of the materials. Given that textiles' mechanical behaviors vary with the direction of stretching in tensile tests, we performed all the mechanical tests in this study in the course direction perpendicular to the textiles' grainline, as jersey fabrics are more elastic in this direction than in the direction of wales[49,50]. The stress-strain

curves illustrated the distinctive mechanical responses displayed by the composites prepared with different fabrication methods (Figure 2c).

We characterized the stress-strain responses of the textile and textile composites by stages (Figure S4). In Stage I, crimp yarns of plain cotton textiles were first straightened before the textiles were extended, and the modulus increased. However, this response was not seen in the composites' curves, which might be because of the presence of the biofilm that increased the friction between the yarns and restrained the stitch loops from changing their shapes. Stage II showed different mechanical behaviors of the tested materials: it was the linear elastic stage with reversible deformation caused by yarns moving within the textile structure for the plain textiles and AS-2 g/mL[49], and the multi-cracking stage for DB-1 mm and VF. By calculating the Young's moduli using the curve in this stage, we found that compared with the plain textiles (~33 kPa), biofilm adsorption increased the modulus by an average of 120% (~74 kPa) (Figure S5). The porous structure of conventional knitted textiles formed by loops can effectively dissipate strain, rendering the textiles extensible and formable substrates in textile-based composites[51,52]. Dry biofilm, on the other hand, is stiffer and more brittle because of curli fibers' rigid structures[44,53,54]. The biofilm coating might have strengthened individual yarns, reduced the pore size, and created yarn-to-yarn adhesion. Hence, as the integration density of the adsorbed biofilm increased with more concentrated biofilm solutions used, the overall strength of the composites was improved (Figure S6). The stress-strain curves of DB-1 mm and VF showed minimal elastic deformation responses up to approximately 10% strain. In contrast, we observed repeated sudden stress drops and rises, a typical behavior of composites in which textiles are added to improve the mechanical performance and durability of inorganic matrices (e.g., textile-reinforced mortar)[55]. Each "spike" in the response represented a crack developed under load on the specimen, and more specifically,

on the biofilm coating. As stress grew, crack propagation was also associated with large strain increases. Although the curves of DB-1 mm and VF had similar shapes in this stage, we noticed that the curve of VF spanned a wider range of strain, indicating that the biofilm was more well-integrated in the textile with vacuum-aided filtration than with doctor blading[56]. In Stage III, all the specimens underwent nonreversible deformation until failure. The plain textiles demonstrated an excellent elongation at break of 400%, which is a result of both the elastic spandex contained in the yarns and the knitted structure of the textiles[57]. Although we expected introducing biofilm to textiles would decrease the elongation due to the same yarn-restraining effect mentioned earlier, vacuum filtration, unlike the other two methods, improved the elongation at break of plain textiles by approximately 140%. Looking at the cross-section of the vacuum-filtered composites, biofilms were found to be deposited into the pores of the textile matrices. After drying, the loss of water in the "filler" biofilm caused the entire textile substrate to shrink. This shrinkage in the material would explain the overall increase in the percentage of elongation when the specimen broke, as it was compared to the initial shrunk state (Figure S7).

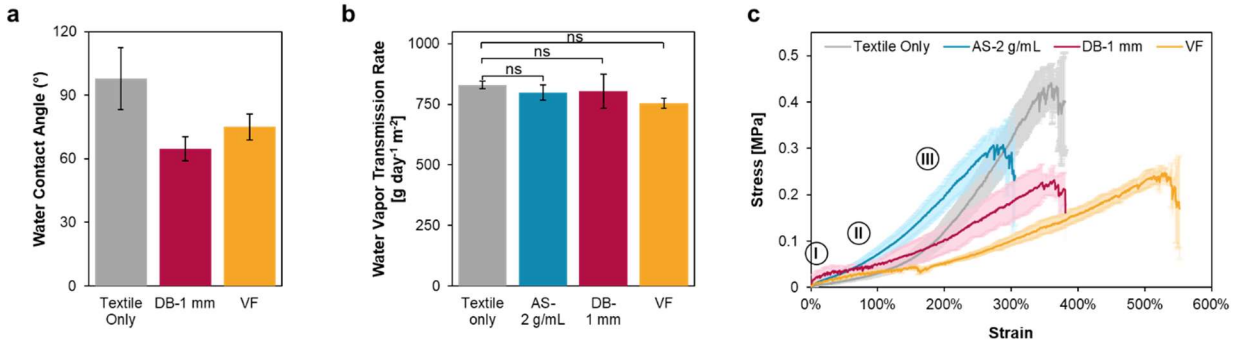

Figure 2. Effect of fabrication method on the physical and mechanical characteristics of biofilm-textile composites. (a) Bar plot of the water contact angle of the plain textile and composites revealing the modified surface wettability after the biofilm coating was introduced. The bars

represent mean values, and the error bars are standard deviations. (b) Bar plot of the WVTR of the plain textile and the composites with the highest integration densities showing retained breathability after integration. The bars represent mean values, and the error bars are standard deviations. (c) Stress-strain curves of the plain textile and composites showing an improved Young's modulus with adsorption (seen in Stage II) and elongation at break with vacuum filtration (seen in Stage III).

Water-Induced Self-repairing in Biofilm-textile Composites

Given that curli and curli-based composites films have been shown to intrinsically self-heal physical damages and recover functionalities after hydration[28,44], we investigated whether integrating curli biofilm can facilitate repairs of macro-sized damages on textiles and enable the composites to regain their mechanical integrity and strength. Here, we employed two types of repairs commonly used for polymeric materials: patching and welding.

Self-repairing by Patching

Patching refers to the process of covering broken materials with new materials or superficial patches[58]. Using native textiles as patches is preferred when repairing textiles in order to restore their original features. We tested the biofilm-textile composites as adhesive patches by cutting 1 cm wide composite strips into two pieces, rehydrating the two ends each with 20 μL of water, and overlapping the ends (with an area of 4 mm × 1 cm) (Figure 3a). After drying, the two pieces of composite were visibly joined into one piece by the overlap region. To visualize the repair mechanism in the overlap region, we imaged its cross section with SEM (Figure 3b). We noticed that the biofilm coating from the two composite pieces healed and held the two pieces together. Specifically, in the adsorption method, the biofilm surrounding individual textile fibers held the yarns closely to each other; whereas in the other two methods, the cross-section images of the

overlap region revealed that the biofilm layers self-healed into one thick layer in between the two composite pieces. This observation was the result of the differences in morphological and integration density stemming from the different integration methods.

To study the performance of the biofilm-textile composites as adhesive patches for repairing damages, we measured the adhesion strength of the composites fabricated by all three methods using a modified version of single lap shear tests (Figure 3c). In traditional lap shear tests, shear forces are applied to separate two adherends that are glued by an adhesive, mimicking a typical failure mode of adhesive joints[59]. In our modified version, the adhesive is the biofilm that has already been integrated throughout each textile piece, not just in the overlap region; and the gluing relies on the self-healing of biofilm. The adhesion strength, defined as the ratio of the maximum load at fracture and the overlap area, was calculated for all the biofilm-textile composites with various integration densities as well as textiles integrated with untransformed bacteria cells made with the same fabrication methods (labeled as AS-Cell, DB-Cell, and VF-Cell). As shown in Figure 3c, overall, the composites with high integration densities reported stronger adhesion. In the overlap region, when a higher density of curli fibers was hydrated and put into contact, more molecular interactions and fiber entanglement were created, which led to healing between the biofilms and the composites[28]. The rise in adhesion strength with increasing integration density of biofilm also agrees with Kendall's mathematical model of crack propagation on lap joint, in which the maximum load is dependent on the elastic modulus and thickness of the adherends and the adhesive energy of the bond[60]. Looking at each fabrication method, we found the adhesion strength of the composites made with biofilm adsorption increased with the integration density when higher biofilm concentration was used, while the doctor-bladed samples with different thicknesses demonstrated adhesion strength comparable to each other. This observation indicated

that doctor-bladed biofilm displayed comparable binding quality to the textile substrate independent of the biofilm load.

When examining the biofilm-textile composites (containing both cells and curli fibers) with textiles integrated with untransformed cells (no curli fiber expression), we first noticed low adhesion strength for AS-Cell-2 g/mL and VF-Cell (1 – 2 kPa) compared to the composites integrated with biofilm (4 – 13 kPa). Although incubating the textiles in 2 g/mL untransformed cell solution resulted in an integration density (~ 16 mg/cm^2) comparable to AS-2 g/mL (14 mg/cm^2), only one out of three specimens tested had its pieces joined. Considering that untransformed cells do not produce curli fibers, this observation indicated the pivotal role of curli fibers in biofilm self-healing. Also, since the untransformed cells were not entangled within curli fiber aggregates as extracellular matrix, they were more likely to penetrate the textile matrix than being adsorbed on the surface, thus unable to generate strong adhesion on the surface. Similarly, when vacuum filtering untransformed bacteria cells, the majority of the cells went through the textile directly and ended up in the filtrate, resulting in a substantially lower integration density (15 mg/cm^2, compared with 25 mg/cm^2 for VF), limiting the adhesion strength.

Contrastingly, the textiles doctor-bladed with the cells (DB-Cell-0.17 mm, DB-Cell-1 mm) displayed adhesion strength values without statistically significant differences with their biofilm-textile composite counterparts. The cell strain we used was derived from MC4100 (LSR10) and does not produce other common extracellular materials apart from curli fibers, such as fimbriae, flagella, cellulose, and lipopolysaccharide O antigen, which have been reported to contribute to the adhesion and/or cohesion of bacterial biofilm[34,61-65]. To understand the reason behind the high adhesion strength of samples prepared by doctor blading untransformed cells, we first calculated the samples' integration density, and noticed greater values compared with the biofilm-textile

composite counterparts (containing both cells and curli fibers) with the same wet thickness. DB-Cell-1 mm achieved a 1.4-fold integration density compared to DB-1 mm, meaning the dry cell layer of the composites may contain a much greater number of cells than the biofilm layer (Figure S8). A recent work making bulk stiff living materials with only PQN4 cells revealed the tight packing of the cells after casting and drying[66]. Furthermore, the characterization of the cast materials in this work suggested that the mechanical integrity was possibly contributed by the materials' heterogeneity resulting from the intracellular components (e.g., nucleic acids, lipids, and proteins) released after cell death[66]. In our case, these compounds might have contributed to cell layers binding to the textile surface and covering the fibers, and to the cohesion reformed between the cell layers of patched composites containing doctor-bladed cells. In addition, the packing and the heterogeneity together allowed the dry cast cells to have high Young's moduli ranging from 5 to 42 GPa, which further aided in the mechanical strength of the composites with doctor-bladed untransformed cells and their high adhesion strength[60,66].

Self-repairing by Welding

Although the adhesive biofilm-textile composite patches provide a simple repairing method and reliable outcomes, closing cuts directly on textiles without overlapping the ends is preferable, particularly for retaining aesthetic features and wearing comfort. Therefore, we explored welding as a second repair method, where we placed the ends of 1 cm wide textile strips that were cut into two together, rehydrated the ends with 40 μL of DI water, and dried the composites until the edges were fused (Figure 3d). The self-healing of biofilm was more challenging with welding than with patching, as the cross-sectional area of the composites (< 0.1 cm^2) was much smaller than the surface area of lap joints (0.4 cm^2). Therefore, we chose to perform welding and the subsequent

mechanical characterization only with the doctor-bladed composites that had the largest cross-sectional area and displayed the highest adhesion strength with the patching method.

All the doctor-bladed biofilm composites were able to fully close the cut through the cohesion of the biofilm layer on the textile's front surface (Figure 3e). To characterize the mechanical strength of the welded composites, we applied tensile loads on the healed cut and recorded the stress at breakage. In general, the composites tested broke at an average stress around ten times smaller than the breaking stress of plain textiles, because breaking the cotton yarns and fibers in plain textiles required large stress. All the doctor-bladed composites, including the untransformed cell-only composite control (DB-Cell-0.17 mm) had breaking stress values comparable with each other, demonstrating a similar quality of cohesion in the biofilm and cell layer (Figure 3f). As explained in the previous section, the cohesion was likely a result of the interfibrillar and intermolecular interactions reformed in the biofilm layer, and the dense packing and heterogeneous compounds in the cell layer.

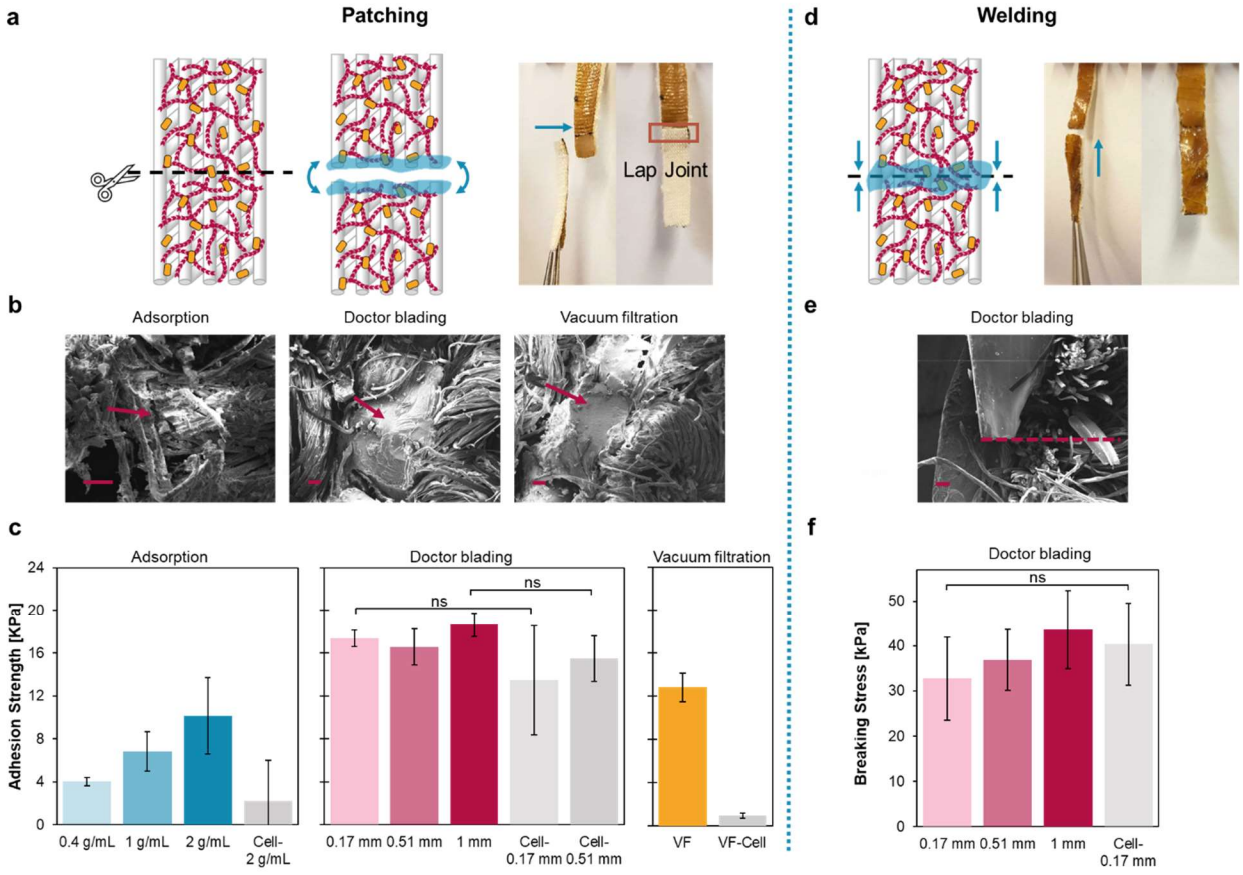

Figure 3. Self-repairing ability of biofilm-textile composites. (a) A schematic and an image showing the steps of using biofilm-textile composites as adhesive patches to repair cuts. (b) SEM images showing that the biofilm reformed in the overlap region joined the two composite pieces. The scale bars are 50 µm. The arrows point at the self-healed biofilm in the lap joints. (c) Adhesion strength obtained from the lap shear tests of the biofilm-textile composites and untransformed cell-only composites repaired by the patching method. The bars represent mean values, and the error bars are standard deviations. (d) A schematic and an image showing the cut repair by welding ends of two biofilm-textile composite pieces. (e) An SEM image of the cross-sectional view of a welded DB-1 mm composite with the textile substrate on the right and the biofilm layer on the left. The red dashed line indicates the cut made with scissors, which was repaired after the two

composite pieces were welded by the cohesion of the biofilm layer. The scale bar is 50 µm. (f) Breaking stress of the composites doctor-bladed with biofilm and untransformed cells (DB-Cell-0.17 mm) obtained from the stress-strain curves. The bars represent mean values, and the error bars are standard deviations.

When examining the composites after their mechanical failure, we noticed that the combination of adhesion and cohesion failure resulted in the mechanical failure in both patched and welded biofilm-textile composites (Figure 4a). At the failure region, the biofilm layer was broken and detached from the textile. We summarized the failure mode in a schematic shown in Figure 4b. In the lap shear test of a patched doctor-bladed composite, the specimen underwent a multi-cracking stage where cracks propagated from the two ends to the center (i.e., the lap joint). The final crack occurred at the edge of the lap joint, where the thickness of the biofilm layer changed due to the biofilm self-healing in the joint, and appeared straight, as shown in Figure 4a (top). Then, the healed biofilm layer was peeled off from one of the two textile substrates under load, leading to an adhesion failure. A similar failure process happened when stress was applied to the welded composites, except that the last crack did not form at a consistent distance to the healed cut. Thus, the biofilm detached from the textile substrate did not have a consistent area, and the stress required to achieve such adhesion failure varied, as indicated by the irregular edge of the biofilm layer in Figure 4a (bottom). To further understand the adhesion failure, we imaged a piece of biofilm layer peeled off from the doctor-bladed composites and saw that the textile fibers covered by the biofilm were also removed from the textile surface (Figure 4c). These fibers protruding from the textile surface were embedded in the deposited biofilm layer, binding the biofilm firmly to the yarns. Therefore, the adhesion strength between the biofilm and the textile was impacted by the number of cotton fibers coated, in other words, the area of adhesion from the last crack to the cut. Since

the composites prepared with doctor-bladed biofilm and those made with untransformed cells both created an even layer of coating over the same textile surface, it was likely that regardless of the layer's thickness, their adhesion strengths were close.

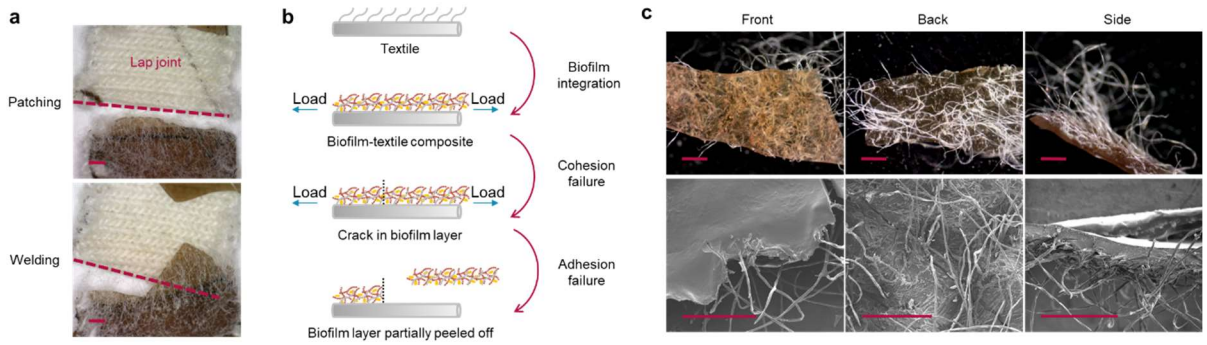

Figure 4. Mechanical failure of self-repaired composites. (a) Optical microscopy images of the patched and welded region of DB-1 mm composites that failed after the mechanical tests. The red dashes indicated the cuts made by scissors, repaired by patching and welding, and reformed after mechanical tests. Under the mechanical load, the biofilm layer from the top composite piece was partially peeled off together with the bottom composite piece from the textile substrate. (b) A schematic illustrating the mechanical failure of the biofilm-textile composites resulted from both the cracking in the biofilm layer (cohesion failure) and the detachment of the layer from the textile (adhesion failure). (c) SEM images showing the front, back, and side view of a biofilm piece peeled off from a doctor-bladed composite covering the textile fibers extruding from the textile surface.

Challenges and Outlook

In this study, we have constructed self-repairing curli-expressing biofilm-textile composites with adsorption, doctor blading, and vacuum filtration. These methods are fast and simple, and can tune the morphological, physical, and mechanical characteristics of the resulting composites. Our results demonstrated that the composites can effectively self-repair visible cuts through patching

and welding, and the strength of the restored sample resulted from the strong cohesion within the biofilm as well as the adhesion between biofilm coatings and textile substrates.

One challenge associated with depositing a biofilm layer on the surface of a soft textile substrate is biofilm buckling. When growing on dry substrates, biofilm forms three-dimensional buckles due to the internal mechanical stress created by the friction between the biofilm and the textile surface. The cohesion of biofilm promotes buckling while the biofilm-textile adhesion facilitates the stress to be transmitted to the textile substrate, initiating the deformation of the composites[67,68]. Providing external stress to the textile substrate can be a solution to reduce deformation. For instance, in this work, we flattened the integrated textiles before drying and kept the edges fixed by taping or clamping during the drying process to reduce wrinkles and buckles.

The biofilm-textile integration methods proposed in this study are deemed applicable in the clothing industry in the future because of the simplicity of fabrication, as well as the composites' retained breathability, enhanced mechanical strength, and effective water-inducible self-repairing ability. To implement such applications, however, we must face the difficulty posed by the long-term stability of biofilm coating during the routine use of biofilm-integrated clothing. For example, the bacteria in the biofilm are not expected to survive the detergents and rotation during laundry processes. A potential solution by *Raab et al.* suggested that dried bacteria or spores can be reloaded after laundry or before usage to regenerate biofilms[11]. Also, prior work on genetically engineered curli fibers vacuum-filtered onto non-woven textiles demonstrated the retention of curli on textiles when exposed to detergents, strong solvents, and constant agitation[38]. Therefore, an alternative solution to maintain the composites' stability can be integrating purified and functionalized curli fibers without the biofilm on textiles to display self-healing and customizable features. We attempted self-repair after producing curli fibers modified to secreted extracellularly

into the culture media, purifying the protein with a method based on vacuum filtration, and doctor blading the product protein hydrogel onto the textiles (0.17 mm wet thickness). The self-healing behavior of the curli adhered on the textiles enabled the patching repair of curli-textile strips, as demonstrated by applying loads on the tensile tester (see Supporting Information Movie S1), highlighting the involvement of curli fibers in the self-repair mechanism of biofilm-textile composites.

To demonstrate the repair size of biofilm-textile composites and the ease of integration, we made two garment prototypes with textiles joined only by the integrated biofilm (Figure 5). We replaced the doctor blading method with an even simpler spreading of the biofilm pellet over the designed overlap region with a spatula. The biofilm integrated with all three methods allowed for the adhesion initiated by rehydration between two composites and between composite and regular plain textiles. These prototypes helped to reveal the potential of biofilm-based self-repair to replace sewing in making garments and maintaining their mechanical integrity.

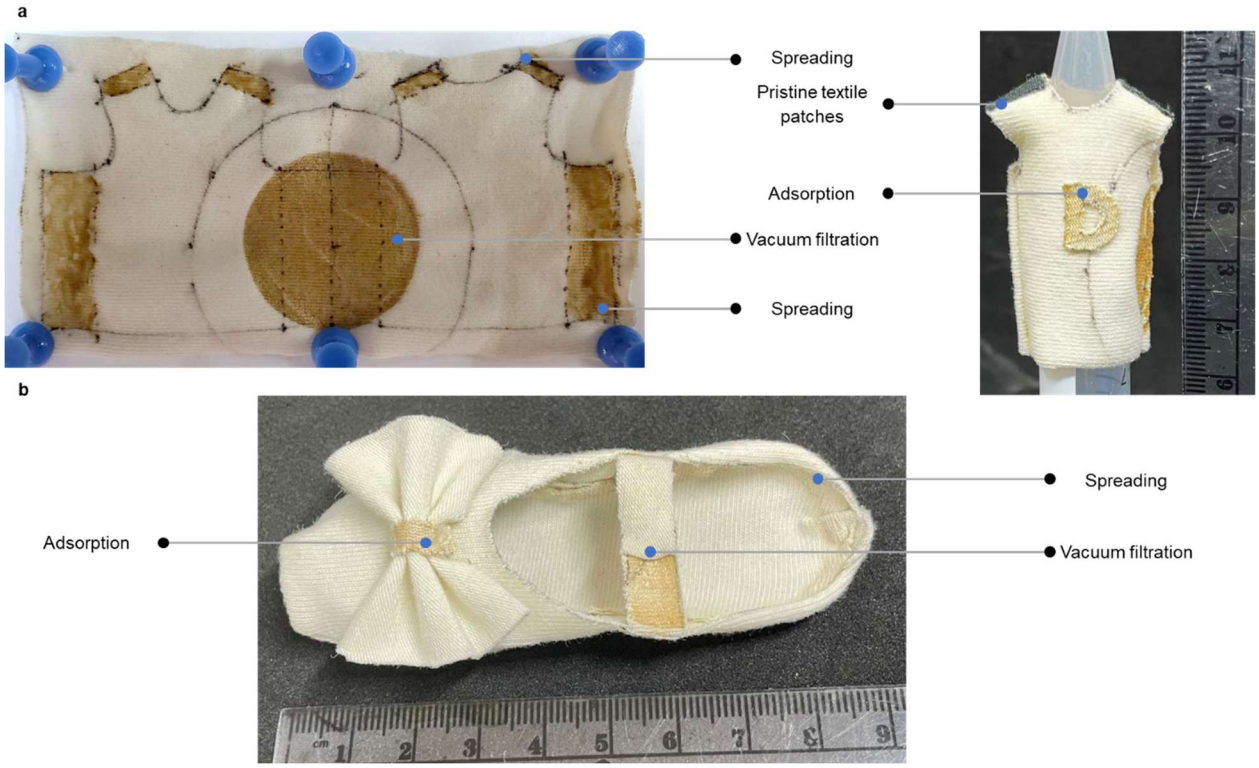

Figure 5. Garment prototypes fabricated based on the repair mechanism of biofilm-textile composites. (a) A mini shirt with an adhesive decoration patch made with biofilm-adsorbed composites in the front and shoulder pads made with regular plain textiles. (b) A mini dance shoe with an adjustable strap utilizing the patching repair of biofilm-textile composites.

The benefits of integrating bacteria biofilm can be maximized by utilizing the living properties of biofilm and displaying novel features through the material. SEM images of the biofilm composites prior to drying revealed that the textile fibers were covered with biofilm-containing bacteria cells (Figure S9). Although some cells might have died during the composite fabrication, we expect the biofilm's living properties can be restored to some extent after a more suitable living condition is provided. In fact, stiff materials made by casting and drying living bacteria cells have demonstrated the preservation of cell viability[66]. Using synthetic biology, these cells could be further engineered to tune the characteristics and adhesion of the biofilm, detect and respond to environmental

stimulations, and display tailored properties to a broad range of applications. Combining the self-healing ability and the living properties, the biofilm-textile composites provide a facile but useful tool to drive the transition towards sustainable production and consumption of textiles and the industry of versatile smart textiles.

Methods

Cell Strains, Plasmids, and Curli Expression

The pET21d-*csgBACEFG* plasmid encoding the entire curli operon, and the *E. coli* mutant strain, PQN4, from which the native curli operon has been deleted were gifted to us by the Joshi Lab (Harvard University, Boston, MA). This plasmid contains a T7 promotor for inducible curli expression, a glycine-serine rich flexible linker $(GSG)_4$, and a six-histidine tag at the C-terminus of CsgA to enable future immunodetection or purification. As a negative control for amyloid expression, a pET21d plasmid containing the *malE* gene encoding the maltose binding protein MBP) was used.

To express the protein, we first transformed the modified plasmid into electrocompetent PQN4 cells, which were then streaked onto a lysogeny broth (LB) agar plate containing 100 µg/mL carbenicillin and 0.5% (m/v) glucose (for catabolite repression of T7 RNA polymerase). As a control, we also streaked untransformed PQN4 cells onto an LB agar plate containing 25 µg/mL chloramphenicol. After overnight incubation at 37°C, one colony was picked from each agar plate and inoculated into a 5 mL LB starter culture containing 100 µg/mL carbenicillin and 2% (m/v) glucose for the transformed cells and 25 µg/mL chloramphenicol for the untransformed cells. The starter cultures were grown overnight in an incubator shaker at 225 rpm and 37°C. The next day, the stationary phase culture of transformed cells was diluted 100-fold in fresh LB media containing 100 µg/mL carbenicillin and cultured at 37°C and 225 rpm for approximately 24 hours to allow

for protein expression. The untransformed cells were also diluted 100-fold with LB media (25 μg/mL chloramphenicol) and grown under the same condition. Both cultures were stopped when the cells reached an optical density at 600 nm of ~4 and centrifuged for 25 min at 4000×*g* for biofilm collection in the pellets. Each 500 mL culture yielded ~3.0 g curli-expressing biofilm pellet or ~2.2 g untransformed *E. coli* cell pellet.

Textiles

The textile samples used in this study (94% cotton and 6% spandex) were knitted jersey fabrics provided by lululemon athletica inc. Knitted textiles have different patterns on their two sides, generated by the stitches in the knitting process. For consistency, we defined the side showing the loops of stitches (usually referred to as "the right side" for knitted fabrics) as the "front" side of the textile and deposited biofilm on this side. The "back" side reported in this study is defined as the side where the ends of the loops can be seen (usually referred to as "the wrong side" for knitted fabrics).

Fabrication of Biofilm-textile Composites

Three methods were used to fabricate composites with the collected biofilm and the textiles: adsorption, doctor blading, and vacuum filtration.

Adsorption of Biofilm on Textiles

The pelleted biofilm from the culture of transformed bacteria was weighed and diluted to 0.4 g/mL, 1 g/mL, and 2 g/mL with deionized (DI) water. The textile samples with a dimension of 6 cm × 6 cm were immersed in 4 mL of biofilm solutions overnight in small petri dishes at room temperature to allow for biofilm adsorption to the textiles. The following day, the textile composites were air dried at room temperature overnight.

Doctor Blading of Biofilm on Textiles

The biofilm pellet was doctor-bladed onto the front side of textiles samples using a glass slide as blade and masks made with one layer of glass coverslip (0.17 mm thick), three layers of glass coverslips (0.51 mm thick), and one layer of glass slide (1 mm thick) coated with a layer of Teflon tape. The composites were then air dried at room temperature overnight.

Vacuum Filtration of Biofilm on Textiles

The textile samples were cut into 7 cm x 9 cm pieces and pre-wetted in LB medium. The biofilm pellet was resuspended in LB to 0.65 g/mL. We performed preliminary tests by varying the biofilm concentration and did not observe any direct relevance between the biofilm concentration and the final amount of biofilm integrated. Knitted textiles have large pore sizes compared to the size of bacteria. To increase the amount of biofilm trapped during vacuum filtration, a polypropylene/polyethylene separator depth filter with 10 μm pores (VWR) was placed under the textile, as we have previously shown that curli fibers formed aggregates and did not pass through filter membranes with such pore size in vacuum filtration[39]. The filtration was stopped until the textile and filter membrane were completely clogged, and no liquid could pass through. Approximately 7 mL biofilm solution with a biofilm concentration of 0.65 g/mL was filtered under vacuum, leaving a layer of biofilm that covered an area of 7.55 cm^2 on the front side of the textiles. The textile composites were air dried at room temperature overnight.

Fabrication of Cell-textile Composites

The pellets from the untransformed bacterial culture were weighed and used to fabricate cell-textile composites using the same three methods described above. In the adsorption method, the biofilm concentration and volume were kept the same. With doctor blading, cell layers of the same

thicknesses were made on the textile surface. Without the curli fibers, the untransformed cells did not aggregate, thus being filtered through the textiles and 10 μm-pore size filter membranes in vacuum filtration. Despite the fact that the textile-filter membrane was not clogged, the concentration of the cell solution and the filtration volume were controlled to be the same as in the fabrication of biofilm-textile composites.

Scanning Electron Microscopy

Scanning electron microscopy (SEM) images were taken for the textile composites prepared with the aforementioned methods and the dry biofilm layer peeled off from the doctor-bladed composites. In particular, to visualize the structure of biofilm coated on the textiles, the composites were treated for 15 minutes each with 25%, 50%, 75%, and 100% v/v ethanol and dried in a critical point dryer (Leica EM CPD300). The rest of the composites and the peeled-off biofilm underwent air drying. All samples were sputter coated with platinum to a thickness of 5 nm (Leica ACE600). The microscopy was performed with a FEI Quanta 450 Environmental Scanning Electron Microscope (Field Electron and Ion Company).

Water Vapor Transmission Test

The dry weights of plain textile samples before biofilm integration (W_t) and the biofilm-textile composites (W_c) were measured with Equinox Analytical Balance (Adam Equipment) for each integration method. The integration density represents the weight of biofilm integrated per unit area of textile. A minimum of three replicates were measured for each method, and the average (in mg/cm^2) was reported.

$$Integration\ Density\ = \frac{W_c - W_t}{Area} \quad (1)$$

Tensile Test

The uniaxial tensile test was performed according to the ASTM D5053-06 method, with slight modifications, using Shimadzu EZ Universal Tensile Tester (Shimadzu), which is equipped with a load cell of 500 N. Strips of 1 cm × 6 cm were cut from the dry biofilm-textile composites and the composites integrated with untransformed PQN4 cells (not curli-producing) made with the three integration methods as well as the plain textile (with no biofilm). The specimens were gripped onto the tensile tester with a gauge length of 2 cm and stretched at a constant speed of 30 mm/min in the direction perpendicular to the textiles' grainline until breakage. The tensile test was also done for the welded doctor-bladed composites at a speed of 10 mm/min. For each type of composite, a minimum of three tests were carried out. The average stress-strain curves were obtained by averaging the calculated stress (MPa) corresponding to every 0.1% strain increment.

Contact Angle Measurement

Contact angles were measured by OCA 15EC (Dataphysics) using DI water droplets of 1 μL on the front side of the plain textile and the biofilm-textile composites. The images were taken and analyzed by ImageJ, and the average contact angles of quadruplicates were calculated.

Self-repair of Composites and Single Lap Shear Test for Composite Patches

The biofilm-textile composites with a dimension of 1 cm × 6 cm were cut in the middle into two pieces using scissors. To heal the cut, the two pieces were joined either by aligning the ends (welding) or by overlapping the ends (patching). In the welding method, the two edges of the cut were placed right next to each other and rehydrated with 40 μL DI water in a petri dish. The composite strips were taped to the petri dish to ensure that the ends were held together while self-healing, and then air dried on the bench. In the patching method, the ends (with a dimension of 1 cm × 4 mm) of the composite pieces were wetted with 20 μL DI water each and then sticked

together with the biofilm-coated side facing toward each other. While the composites were air dried on the bench, the two ends were kept in contact by placing a 25 mm × 75 mm glass microscope slide on the top of the overlap region.

To characterize the adhesion strength of the textile composite patches, which is calculated by dividing the maximum force applied by the adhesion area, single lap shear tests were carried out using Shimadzu EZ Universal Tensile Tester (Shimadzu). The self-repaired specimens were gripped, and the distance between the two grips was controlled to be 2 cm for all the tests. A shear rate of 30 mm/min was applied until the healed two pieces were pulled apart. Quadruplicates were done for each integration method, and the average adhesion strength values were calculated.

The same lap shear test was performed with the cell-textile composites made with the three methods using untransformed cells, except for the specimens that remained as two pieces after being dried (Adhesion Strength = 0 kPa).

$$Adhesion\ Strength = \frac{F_{max}}{Adhesion\ Area} \quad (3)$$

Statistics

Paired t-tests were performed on SPSS Statistics (IBM) to compare (1) the WVTR of biofilm-textile composites made with each of the three methods with the rate of the plain textiles, (2) the Young's modulus of plain textiles and AS-2 g/L composites, (3) the adhesion strength of patched DB-0.17 mm and DB-1 mm with the strength of composites made with untransformed cells, and (4) the breaking stress of welded DB-0.17 mm with that of the cell-textile composites. A probability (p-value) less than 0.05 was considered significant. $p > 0.05$ was denoted as "not significant" (ns).

Fabrication of Textile Composites with Purified Curli Fibers

Curli fibers were expressed with PQN4 cells and the same plasmid encoding curli operon with *csgB* gene deleted to enable curli fibers to be secreted into the medium. Then, the curli fibers were harvested in a hydrogel form from the medium following a vacuum filtration-based purification method we previously established[39]. The curli fibers were doctor-bladed onto the textile with a 0.17 mm thick mask and dried at room temperature overnight.

References

1 The price of fast fashion. *Nature Climate Change* **8**, 1-1 (2018). https://doi.org/10.1038/s41558-017-0058-9

2 EEA. Textiles and the environment: the role of design in Europe's circular economy. *EEA Briefing Fe 10/2020, European Environment Agency* (2022). https://doi.org/10.2800/006659

3 Laitala, K., Boks, C. & Klepp, I. G. Making Clothing Last: A Design Approach for Reducing the Environmental Impacts. *International Journal of Design* **9**, 93-107 (2015).

4 Ramesh, S. *et al.* Self-healing and repair of fabrics: A comprehensive review of the application toolkit. *Materials Today* **54**, 90-109 (2022). https://doi.org /10.1016/j.mattod.2021.11.016

5 Zhou, H., Wang, H., Niu, H. & Lin, T. Recent Progress in Durable and Self-Healing Super-Nonwettable Fabrics. *Advanced Materials Interfaces* **5**, 1800461 (2018). https:// doi.org/10.1002/admi.201800461

6 Lindstrom, A. B., Strynar, M. J. & Libelo, E. L. Polyfluorinated Compounds: Past, Present, and Future. *Environmental Science & Technology* **45**, 7954-7961 (2011). https://doi.org/10.1021/es2011622

7 Li, Y., Ge, B., Men, X., Zhang, Z. & Xue, Q. A facile and fast approach to mechanically stable and rapid self-healing waterproof fabrics. *Composites Science and Technology* **125**, 55-61 (2016). https://doi.org/10.1016/j.compscitech.2016.01.021

8 Zhou, H. *et al.* Superstrong, Chemically Stable, Superamphiphobic Fabrics from Particle-Free Polymer Coatings. *Advanced Materials Interfaces* **2**, 1400559 (2015). https://doi.org/10.1002/admi.201400559

9 Saldanha, D. J., Cai, A. & Dorval Courchesne, N.-M. The Evolving Role of Proteins in Wearable Sweat Biosensors. *ACS Biomaterials Science & Engineering* (2021). https://doi.org/10.1021/acsbiomaterials.1c00699

10 Gaddes, D. *et al.* Self-Healing Textile: Enzyme Encapsulated Layer-by-Layer Structural Proteins. *ACS Applied Materials & Interfaces* **8**, 20371-20378 (2016). https://doi.org/10.1021/acsami.6b05232

11 Raab, N. *et al.* A symbiotic-like biologically-driven regenerating fabric. *Scientific Reports* **7**, 8528 (2017). https://doi.org/10.1038/s41598-017-09105-4

12 Dyck, M. K., Lacroix, D., Pothier, F. & Sirard, M.-A. Making recombinant proteins in animals – different systems, different applications. *Trends in Biotechnology* **21**, 394-399 (2003). https://doi.org/10.1016/S0167-7799(03)00190-2

13 Flemming, H.-C. & Wingender, J. The biofilm matrix. *Nature Reviews Microbiology* **8**, 623-633 (2010). https://doi.org/10.1038/nrmicro2415

14 Hemmatian, T., Lee, H. & Kim, J. Bacteria Adhesion of Textiles Influenced by Wettability and Pore Characteristics of Fibrous Substrates. *Polymers-Basel* **13**, 223 (2021). https://doi.org/10.3390/polym13020223

15 Moser, F., Tham, E., González, L. M., Lu, T. K. & Voigt, C. A. Light-Controlled, High-Resolution Patterning of Living Engineered Bacteria Onto Textiles, Ceramics, and Plastic. *Advanced Functional Materials* **29**, 1901788 (2019). https://doi.org/10.1002/adfm.201901788

16 Wang, W. *et al.* Harnessing the hygroscopic and biofluorescent behaviors of genetically tractable microbial cells to design biohybrid wearables. *Science Advances* **3**, e1601984 (2017). https://doi.org/10.1126/sciadv.1601984

17 Prigent-Combaret, C. *et al.* Developmental pathway for biofilm formation in curli-producing Escherichia coli strains: role of flagella, curli and colanic acid. *Environmental Microbiology* **2**, 450-464 (2000). https://doi.org/10.1046/j.1462-2920.2000.00128.x

18 Hung, C. *et al.* Escherichia coli biofilms have an organized and complex extracellular matrix structure. *mBio* **4**, e00645-00613 (2013). https://doi.org/10.1128/mBio.00645-13

19 Tursi, S. A. & Tükel, Ç. Curli-Containing Enteric Biofilms Inside and Out: Matrix Composition, Immune Recognition, and Disease Implications. *Microbiology and Molecular Biology Reviews* **82**, e00028-00018 (2018). https://doi.org/10.1128/MMBR.00028-18

20 Nguyen, P. Q., Botyanszki, Z., Tay, P. K. R. & Joshi, N. S. Programmable biofilm-based materials from engineered curli nanofibres. *Nature Communications* **5**, 4945 (2014). https://doi.org/10.1038/ncomms5945

21 Botyanszki, Z., Tay, P. K. R., Nguyen, P. Q., Nussbaumer, M. G. & Joshi, N. S. Engineered catalytic biofilms: Site-specific enzyme immobilization onto E. coli curli nanofibers. *Biotechnology and Bioengineering* **112**, 2016-2024 (2015). https://doi.org/10.1002/bit.25638

22 Wang, Y. *et al.* Living materials fabricated via gradient mineralization of light-inducible biofilms. *Nature Chemical Biology* **17**, 351-359 (2021). https://doi.org/10.1038/s41589-020-00697-z

23 Praveschotinunt, P. *et al.* Probiotic Associated Therapeutic Curli Hybrids (PATCH). *bioRxiv*, 464966 (2018). https://doi.org/10.1101/464966

24 Duraj-Thatte, A. M. *et al.* Genetically Programmable Self-Regenerating Bacterial Hydrogels. *Advanced Materials* **31**, 1901826 (2019). https://doi.org/10.1002/adma.201901826

25 Schleeger, M. *et al.* Amyloids: From molecular structure to mechanical properties. *Polymer* **54**, 2473-2488 (2013). https://doi.org/10.1016/j.polymer.2013.02.029

26 Knowles, T. P. J. & Mezzenga, R. Amyloid Fibrils as Building Blocks for Natural and Artificial Functional Materials. *Advanced Materials* **28**, 6546-6561 (2016). https://doi.org/10.1002/adma.201505961

27 Duraj-Thatte, A. M. *et al.* Water-processable, biodegradable and coatable aquaplastic from engineered biofilms. *Nature Chemical Biology* (2021). https://doi.org/10.1038/s41589-021-00773-y

28 Huyer, C. *et al.* Fabrication of Curli Fiber-PEDOT:PSS Biomaterials with Tunable Self-Healing, Mechanical, and Electrical Properties. *ACS Biomaterials Science & Engineering* (2022). https://doi.org/10.1021/acsbiomaterials.1c01180

29 Li, J. & Zhang, F. Amyloids as Building Blocks for Macroscopic Functional Materials: Designs, Applications and Challenges. *Int J Mol Sci* **22**, 10698 (2021). https://doi.org/10.3390/ijms221910698

30 Toksoz, S., Acar, H. & Guler, M. O. Self-assembled one-dimensional soft nanostructures. *Soft Matter* **6**, 5839-5849 (2010). https://doi.org/10.1039/C0SM00121J

31 Branco, M. C., Nettesheim, F., Pochan, D. J., Schneider, J. P. & Wagner, N. J. Fast Dynamics of Semiflexible Chain Networks of Self-Assembled Peptides. *Biomacromolecules* **10**, 1374-1380 (2009). https://doi.org/10.1021/bm801396e

32 Knowles, T. P. *et al.* Role of intermolecular forces in defining material properties of protein nanofibrils. *Science* **318**, 1900-1903 (2007). https://doi.org/10.1126/science.1150057

33 Stephanopoulos, N., Ortony, J. H. & Stupp, S. I. Self-assembly for the synthesis of functional biomaterials. *Acta Mater* **61**, 912-930 (2013). https://doi.org/10.1016/j.actamat.2012.10.046

34 Evans, M. L. & Chapman, M. R. Curli biogenesis: Order out of disorder. *Biochimica et Biophysica Acta (BBA) - Molecular Cell Research* **1843**, 1551-1558 (2014). https://doi.org/10.1016/j.bbamcr.2013.09.010

35 Qiang, S., Chen, K., Yin, Y. & Wang, C. Robust UV-cured superhydrophobic cotton fabric surfaces with self-healing ability. *Materials & Design* **116**, 395-402 (2017). https://doi.org/10.1016/j.matdes.2016.11.099

36 Garrett, T. R., Bhakoo, M. & Zhang, Z. Bacterial adhesion and biofilms on surfaces. *Progress in Natural Science* **18**, 1049-1056 (2008). https://doi.org/10.1016/j.pnsc.2008.04.001

37 Ko, J., Jee, S., Lee, J. H. & Kim, S. H. High durability conductive textile using MWCNT for motion sensing. *Sensors and Actuators A: Physical* **274**, 50-56 (2018). https://doi.org/10.1016/j.sna.2018.02.037

38 Saldanha, D. J., Abdali, Z., Modafferi, D., Janfeshan, B. & Dorval Courchesne, N.-M. Fabrication of fluorescent pH-responsive protein–textile composites. *Scientific Reports* **10**, 13052 (2020). https://doi.org/10.1038/s41598-020-70079-x

39 Dorval Courchesne, N.-M., Duraj-Thatte, A., Tay, P. K. R., Nguyen, P. Q. & Joshi, N. S. Scalable Production of Genetically Engineered Nanofibrous Macroscopic Materials via Filtration. *ACS Biomaterials Science & Engineering* **3**, 733-741 (2017). https://doi.org/10.1021/acsbiomaterials.6b00437

40 Dorval Courchesne, N.-M. *et al.* Biomimetic engineering of conductive curli protein films. *Nanotechnology* **29**, 454002 (2018). https://doi.org/10.1088/1361-6528/aadd3a

41 Ashby, M. F. Criteria for selecting the components of composites. *Acta Metallurgica et Materialia* **41**, 1313-1335 (1993). https://doi.org/10.1016/0956-7151(93)90242-K

42 Ullah, H. M. K. *et al.* A review of noteworthy/major innovations in wearable clothing for thermal and moisture management from material to fabric structure. *Textile Research Journal* **92**, 3351-3386 (2022). https://doi.org/10.1177/00405175211027799

43 Tang, K.-P. M., Kan, C.-W. & Fan, J.-t. Evaluation of water absorption and transport property of fabrics. *Textile Progress* **46**, 1-132 (2014). https://doi.org/10.1080/00405167.2014.942582

44 Duraj-Thatte, A. M. *et al.* Water-processable, biodegradable and coatable aquaplastic from engineered biofilms. *Nature Chemical Biology* **17**, 732-738 (2021). https://doi.org/10.1038/s41589-021-00773-y

45 Hsieh, Y.-L. Liquid Transport in Fabric Structures. *Textile Research Journal* **65**, 299-307 (1995). https://doi.org/10.1177/004051759506500508

46 Krainer, S. & Hirn, U. Contact angle measurement on porous substrates: Effect of liquid absorption and drop size. *Colloids and Surfaces A: Physicochemical and Engineering Aspects* **619**, 126503 (2021). https://doi.org/10.1016/j.colsurfa.2021.126503

47 Indushekar, R., Awasthi, P., Gupta, R. K. & Kotresh, T. M. Studies on Test Methods used to Measure Water Vapor Transmission of Fabrics by DSC and Conventional Dish Techniques. *Journal of Industrial Textiles* **34**, 223-242 (2005). https://doi.org/10.1177/1528083705051454

48 Park, G. B., Courtney, J. M., McNair, A. & Gaylor, J. D. S. The Design and Evaluation of a Burn Wound Covering. *Engineering in Medicine* **7**, 11-15 (1978). https://doi.org/10.1243/emed_jour_1978_007_006_02

49 Adolphe, D. C. & Dolez, P. I. in *Advanced Characterization and Testing of Textiles* (eds Patricia Dolez, Olivier Vermeersch, & Valério Izquierdo) 25-57 (Woodhead Publishing, 2018).

50 Jovanović, T., Penava, Ž. & Vrljičak, Z. Impact of the Elastane Percentage on the Elastic Properties of Knitted Fabrics under Cyclic Loading. *Materials* **15**, 6512 (2022). https://doi.org/10.3390/ma15196512

51 Ma, P., Hu, H., Zhang, Y., Sun, B. & Gu, B. Frequency features of co-woven-knitted fabric (CWKF) composite under tension at various strain rates. *Composites Part A: Applied Science and Manufacturing* **42**, 446-452 (2011). https://doi.org/10.1016/j.compositesa.2010.12.016

52 Gao, Y., Xie, C. & Zheng, Z. Textile Composite Electrodes for Flexible Batteries and Supercapacitors: Opportunities and Challenges. *Advanced Energy Materials* **11**, 2002838 (2021). https://doi.org/10.1002/aenm.202002838

53 Ruggeri, F. S. *et al.* Influence of the β-Sheet Content on the Mechanical Properties of Aggregates during Amyloid Fibrillization. *Angewandte Chemie International Edition* **54**, 2462-2466 (2015). https://doi.org/10.1002/anie.201409050

54 Romero, D., Aguilar, C., Losick, R. & Kolter, R. Amyloid fibers provide structural integrity to Bacillus subtilis biofilms. *Proceedings of the National Academy of Sciences* **107**, 2230-2234 (2010). https://doi.org/10.1073/pnas.0910560107

55 De Santis, S., Carozzi, F. G., de Felice, G. & Poggi, C. Test methods for Textile Reinforced Mortar systems. *Composites Part B: Engineering* **127**, 121-132 (2017). https://doi.org/10.1016/j.compositesb.2017.03.016

56 Zhou, F. *et al.* Uniaxial Tensile Behavior of Carbon Textile Reinforced Mortar. *Materials* **12**, 374 (2019). https://doi.org/10.3390/ma12030374

57 Tadesse, M. G. *et al.* Electrically conductive highly elastic polyamide/lycra fabric treated with PEDOT:PSS and polyurethane. *Journal of Materials Science* **54**, 9591-9602 (2019). https://doi.org/10.1007/s10853-019-03519-3

58 Wu, D. Y., Meure, S. & Solomon, D. Self-healing polymeric materials: A review of recent developments. *Progress in Polymer Science* **33**, 479-522 (2008). https://doi.org/10.1016/j.progpolymsci.2008.02.001

59 Wang, Y., Nian, G., Yang, X. & Suo, Z. Lap shear of a soft and elastic adhesive. *Mechanics of Materials* **158**, 103845 (2021). https://doi.org/10.1016/j.mechmat.2021.103845

60 Kendall, K. Crack propagation in lap shear joints. *Journal of Physics D: Applied Physics* **8**, 512 (1975). https://doi.org/10.1088/0022-3727/8/5/010

61 Tay, P. K. R., Nguyen, P. Q. & Joshi, N. S. A Synthetic Circuit for Mercury Bioremediation Using Self-Assembling Functional Amyloids. *ACS Synthetic Biology* **6**, 1841-1850 (2017). https://doi.org/10.1021/acssynbio.7b00137

62 Spurbeck, R. R. *et al.* Fimbrial Profiles Predict Virulence of Uropathogenic Escherichia coli Strains: Contribution of Ygi and Yad Fimbriae. *Infection and Immunity* **79**, 4753-4763 (2011). https://doi.org/10.1128/IAI.05621-11

63 Pesavento, C. *et al.* Inverse regulatory coordination of motility and curli-mediated adhesion in Escherichia coli. *Genes Dev* **22**, 2434-2446 (2008). https://doi.org/10.1101/gad.475808

64 Biesecker, S. G., Nicastro, L. K., Wilson, R. P. & Tükel, Ç. The Functional Amyloid Curli Protects Escherichia coli against Complement-Mediated Bactericidal Activity. *Biomolecules* **8** (2018). https://doi.org/10.3390/biom8010005

65 Beloin, C., Roux, A. & Ghigo, J.-M. in *Bacterial Biofilms* (ed Tony Romeo) 249-289 (Springer Berlin Heidelberg, 2008).

66 Manjula-Basavanna, A., Duraj-Thatte, A. M. & Joshi, N. S. Robust Self-Regeneratable Stiff Living Materials Fabricated from Microbial Cells. *Adv Funct Mater* **31**, 2010784 (2021). https://doi.org/10.1002/adfm.202010784

67 Cont, A., Rossy, T., Al-Mayyah, Z. & Persat, A. Biofilms mechanically damage epithelia by buckling. *bioRxiv*, 2020.2001.2029.923060 (2020). https://doi.org/10.1101/2020.01.29.923060

68 Ziege, R. *et al.* Adaptation of Escherichia coli Biofilm Growth, Morphology, and Mechanical Properties to Substrate Water Content. *ACS Biomaterials Science & Engineering* **7**, 5315-5325 (2021). https://doi.org/10.1021/acsbiomaterials.1c00927

Supporting Information

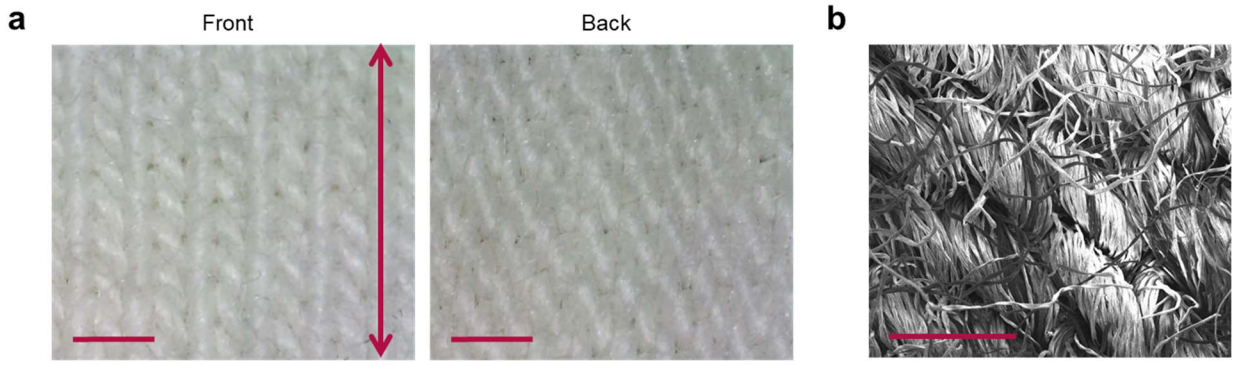

Figure S1. The cotton-spandex knitted textile used as the substrate of the biofilm-textile composites. (a) Optical microscope images showing the knitted features of the front and back sides of the textile. The red arrow aligns with the grainline of the knitted textile, with the arrows pointing toward the wale direction. The scale bars are 1 mm. (b) An SEM image showing that the textile was knitted with yarns that have an average diameter of ~200 µm and consist of fibers ~16 µm in diameter. The scale bar is 500 µm.

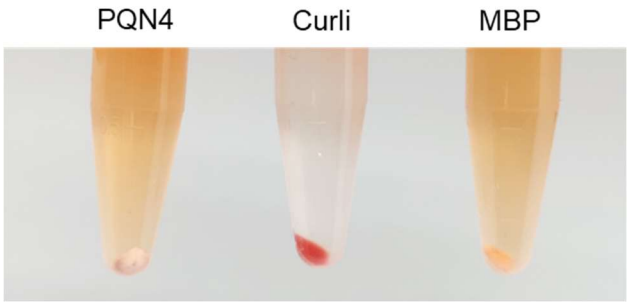

Figure S2. Results of the Congo Red binding assay revealing that amyloid curli fibers have been produced in the biofilm and bound to Congo Red to form a red pellet. The cultures of untransformed PQN4 cells and the cells producing maltose binding protein (MBP) used as controls both showed white pellets and red supernatant.

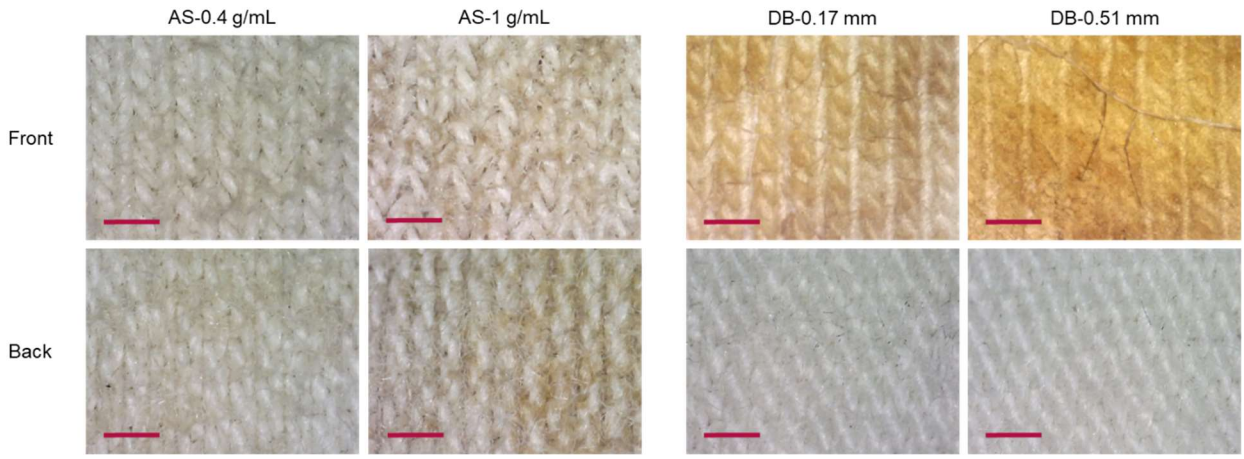

Figure S3. Optical microscope images showing the biofilm distribution on the biofilm-textile composites made by varying the concentration of the biofilm solution (adsorption) and the thickness of the mask (doctor blading). The scale bars are 1 mm.

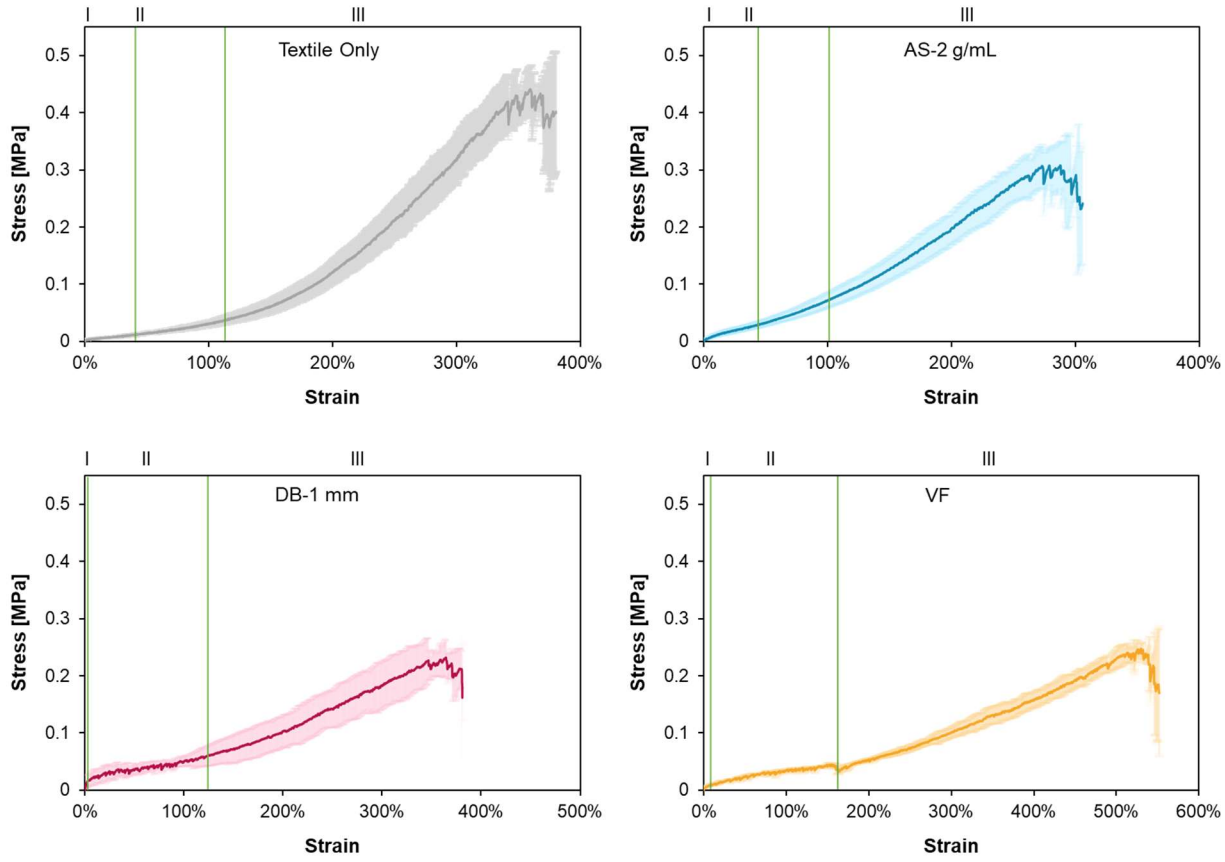

Figure S4. The three stages of the stress-strain responses identified for the textile and the biofilm-textile composites.

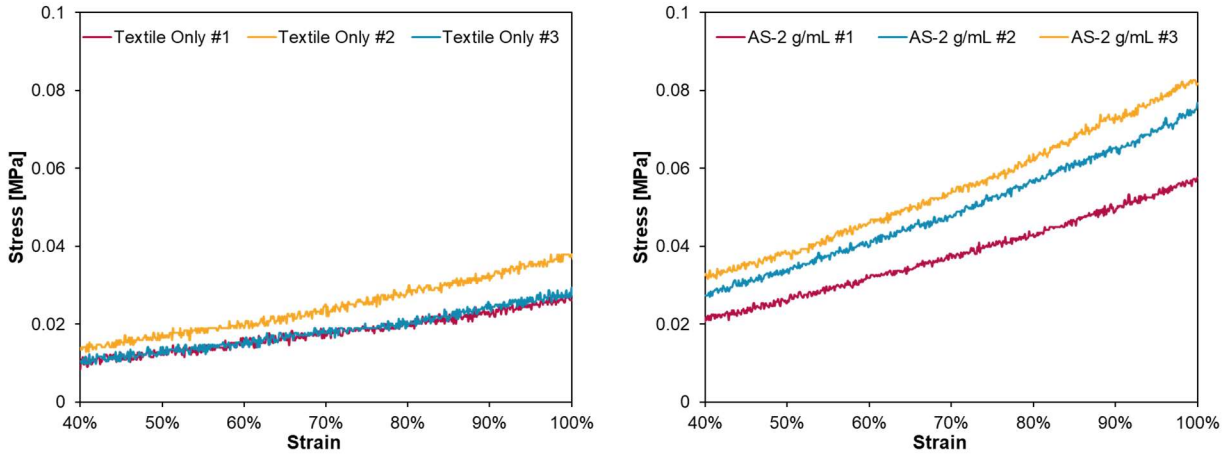

Figure S5. The elastic stage (Stage II) of the stress-strain curves plotted for the triplicates of plain textiles and the AS-2 g/mL composites. The Young's moduli of the specimens calculated based on this section of the curve suggested that the biofilm adsorption with 2 g/mL biofilm solution significantly improved the modulus of the textile ($p<0.05$).

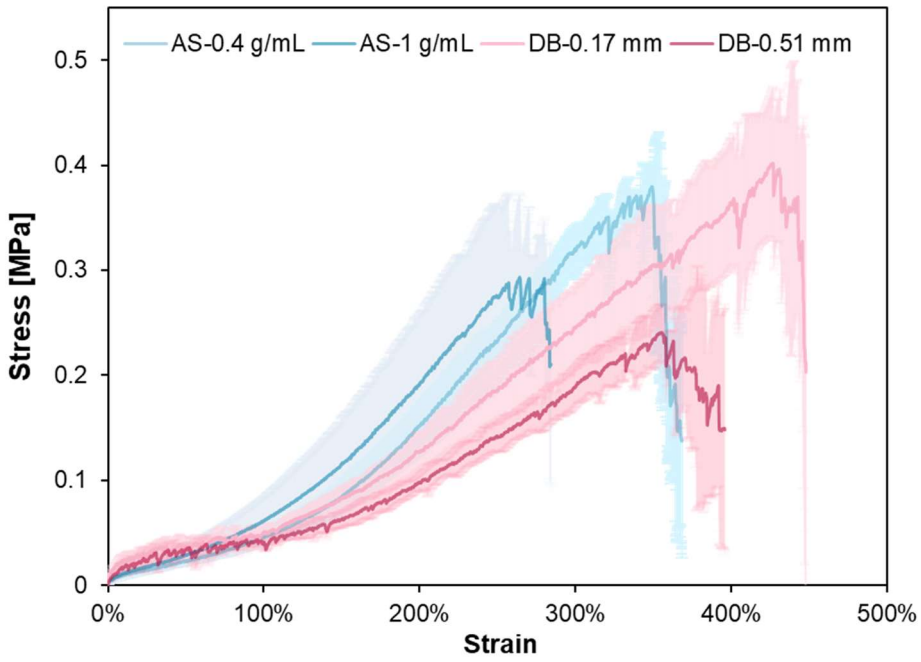

Figure S6. Stress-strain curves illustrating the evolving mechanical responses (Young's modulus, elongation at breakage) of the biofilm-textile composites as the integration density changed.

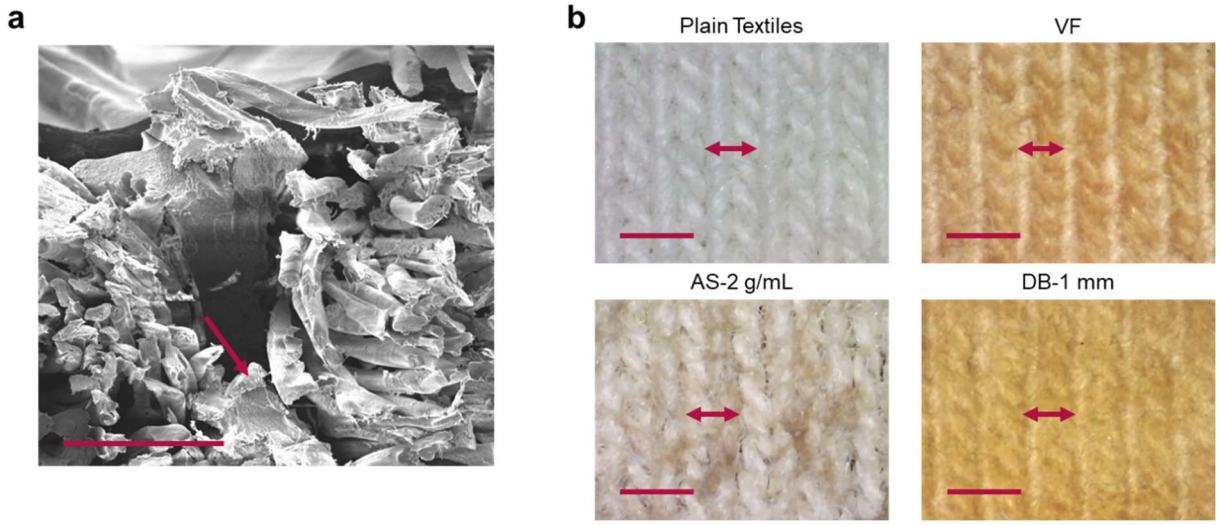

Figure S7. Images revealing the impacts of vacuum-filtered biofilm on the elongation of break of the composites. (a) An SEM image of the cross-section of a VF composite showing the biofilm entrapped in the porous textile matrix. The red arrow points at a cluster of biofilm formed in between the textile fibers. The scale bar is 100 µm. (b) Optical microscope images demonstrating the shrinkage in size after the fabrication of the VF composite. The distance from the left edge of a grainline to that of the next grainline (indicated by the double-headed arrows) was reduced from ~0.75 mm to ~0.61 mm. The distance was measured by averaging the total distance spaced by six adjacent grainlines. As a comparison, the distance was ~0.77 mm for AS-2 g/mL and ~0.66 mm for DB-1 mm. The scale bars are 1 mm.

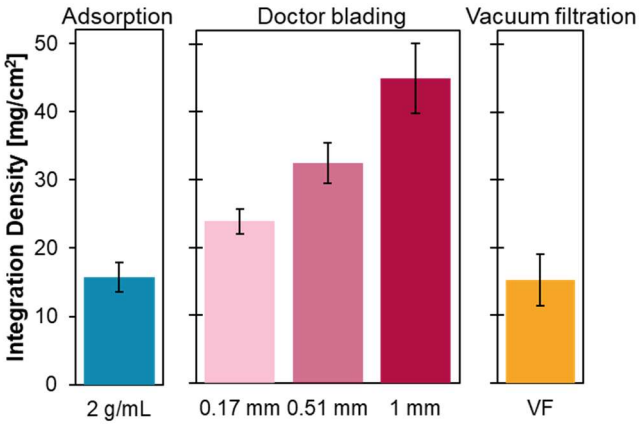

Figure S8. Bar plot of integration density calculated for cell-textile composites prepared using the same three methods discussed and untransformed cells. The bars represent mean values, and the error bars are standard deviations.

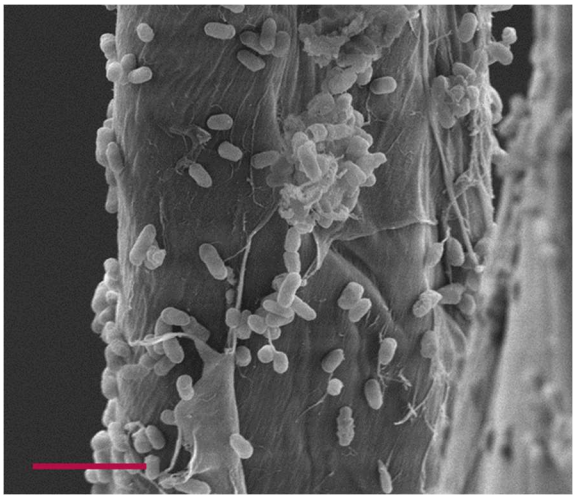

Figure S9. An SEM image showing the bacteria cells and biofilm adsorbed on a single textile fiber. The scale bar is 5 μm.

Movie S1. A movie showing the self-repairing of textile patches doctor-bladed with purified curli fibers (integration density of 0.8 mg/cm^2).

Chapter 4. Discussion and Conclusion

In this thesis, we explored the approaches to enhance the performance and functions of traditional textiles in a sustainable manner. We fabricated biofilm-textile composites by integrating curli-expressing *E. coli* biofilms into knitted cotton textiles with three facile and scalable techniques. These composites have demonstrated high performance in their mechanical strength and their ability to self-repair centimeter-scale cuts after water was introduced.

Chapter 1 highlighted our project's objective to develop textile composites that have high performance and "smart" functions. Inspired by the mechanical stability, processability, and tunability of curli-expressing biofilms from *E. coli*, we chose to integrate the biofilms into regular textiles and allow the resulting composites to display improved mechanical properties and the ability to self-repair mechanical defects.

In Chapter 2, we discussed our motivation to develop the textile's self-repairability by introducing the eco-design requirements in the textile industry proposed to mitigate the industry's negative environmental impacts. We reviewed the research progress on self-repairing strategies and focused on the most extensively studied repair agent, fluorine-based compounds. We discussed their performance in repairing various types of textile defects and pointed out their limitations in the size scale of repair and the scalability of production, as well as the environmental and health concerns associated with the composites' production processes. Then, we introduced the environmental and functional benefits of biologically-derived repair agents like proteins, the previous success with SRT, and the limitations linked to the industrial production of recombinant SRT-like structural proteins. To address these limitations, we proposed the use of *E. coli* biofilms as an ELM for fabricating high-performance textile composites. The mechanical stability, adhesion to various surfaces, processability, tunability, and living properties of biofilms render the material

desired for constructing smart composites when combined with inorganic scaffolds. Furthermore, various characteristics can be displayed through *E. coli* biofilms through the amyloid curli fibers, including curli's native properties (e.g., mechanical robustness, resistance to the harsh environment, and self-healing) and novel programmed properties.

In Chapter 3, we described how we fabricated biofilm-textile composites by integrating *E. coli* biofilms containing extracellularly secreted curli fibers into conventional knitted cotton textiles through three simple, scalable methods: adsorption, doctor blading, and vacuum filtration. We found that the composites had improved mechanical properties (i.e., Young's modulus and elongation at break) and maintained the textiles' breathability. When used as adhesive patches or welded after rehydration, the composites demonstrated the ability to effectively self-repair centimeter-sized cuts. By using the three different fabrication methods and varying the amount of biofilm integrated into per unit area of textile, we also tuned the composites' characteristics and self-repair quality, the latter of which we found was associated with the cohesion and substrate adhesion of the biofilm layer formed.

The three methods we adopted integrated 5 – 32 mg biofilm into per cm^2 of textile, thanks to biofilms' ability to adhere to textile surfaces. When biofilms were initially introduced to a surface, their surface adhesion was reversible and is thought to be associated with the tethering of bacterial surface appendages, surface thermodynamics, Lifshitz-van der Waals interactions, electrostatic-double layer interactions, and acid-base binding[121,122]. As the interfacial water was removed, closer contact and more acid-base interactions between the biofilm and the substrate were enabled[121,123]. At the same time, the bacterial fimbriae, such as curli, generated more tethers to the substrate, strengthening the biofilm-substrate attachment[124,125]. Therefore, the biofilm's adhesion became irreversible. From the substrate perspective, biofilm's adhesion is affected by textiles' hydrophobic

and hygroscopic properties, porous structure, and the roughness of textile surface and fibers[37,86]. Therefore, testing the composite fabrication with textiles made with different materials, weaving methods, and porosity can be interesting in the future to understand the biofilm's adhesion to textile surface and tune the composites' overall performances.

We chose the three methods to fabricate the biofilm-textile composites to allow for scale-up and minimize damage to the biofilms' integrity and viability. The results showed that these three methods led to the different biofilm distribution, wettability, and mechanical properties of the composites. Adsorption resembles the simple and low-cost dip coating technique commonly used to introduce one or multiple compounds from a homogeneous solution to modify substrate surfaces[126]. We immersed textiles in biofilm solutions overnight at room temperature so that the textiles were fully infiltrated, and the biofilms were irreversibly adsorbed on both surfaces of the textile as well as in the textile matrix[126,127]. The infiltration of biofilms might also have impacted the textile's surface roughness, thus enabling rapid water absorption in the water contact angle tests. Other than changing the concentration of the coating solution used, the morphology and the integration density of the biofilm coating can also be tuned by changing the immersion time, the evaporation conditions of the coating solution, and the number of coating cycles[126]. In textile manufacturing, a similar process called "sizing", where yarns are dipped in sizing agent solutions, is widely used to enhance the yarns' mechanical strength for subsequent weaving processes[128]. Similarly, we observed an improved Young's modulus when applying a tensile load to the composites made with biofilm adsorption. Doctor blading is a rapid film-forming technique allowing for controllable coating thicknesses[129]. This process can be done both manually using masks made of tape[130] or glass slides[131], and automatically using a commercial machine with controlled blade speed and micrometer-scale precision of thickness[132] or a simple automatic film

applicator[133]. By using glass slides of different thicknesses as the mask, we varied the wet thickness of the coating and created a smooth layer of biofilm on one surface of the textile. Compared to the other two methods, doctor blading allowed large quantities of biofilm (17 – 32 mg) to be rapidly loaded onto one side of the textile, without affecting the aesthetic features or the properties of the textile on the other side. The high integration density and surface coverage were advantageous in both the patching and the welding methods when repairing the composites, owing to the high cohesive strength in the biofilm layer and the high adhesive strength between the biofilm layer and the substrate. Filtration assisted by vacuum is a common method in the analysis[134,135], isolation[31,107], and composite fabrication[30,136-140] of amyloid fibrils, such as curli fibers and β-lactoglobulin, because these proteins are mechanically strong and stable under vacuum suction and detergents. The applicability of vacuum filtration in making biofilm-textile composites also relies on the dispersion of biofilm in bacterial culture medium and the adhesion of biofilm on textiles[137,141]. The simple and scalable vacuum filtration promotes the formation of composites with layered structures, whose thickness can be tuned by varying the volume of the filtration solution[138]. However, as textiles have larger pore sizes than the filter membranes previously used for composites fabrication with amyloids (pore size of 0.2 μm) [138], we chose to end the filtration until the textile was completely clogged by biofilms to achieve uniform coverage of biofilms. This method forced the biofilm to be trapped in the pores of the textile matrix under vacuum, thereby depositing a layer of biofilm on one surface of the textile, creating the shrinkage of the textile matrix after the composites were dried, and increasing the elongation at break of the composites.

We quantified the amount of biofilm integrated by calculating the mass of biofilms per unit area of textile (i.e., integration density) instead of the thickness of the biofilm layer/coating. To calculate the stress from the tensile test results, we measured the thickness of the composite

specimens using a caliber, which was prone to errors; whereas the standard test method (ASTM D1777-96(2019)) requires textiles' thickness to be measured under a constant pressure applied over the entire surface area of textile specimens[142]. An alternative method to measure the biofilm coating's thickness can be using electron microscopy and imaging the cross-section of the composite textiles/fibers, as reported in previous works on fabric coating[56,143]. However, this method was found challenging in practice, as cutting the composites with scissors during specimen preparation compressed the textiles fibers and the biofilm layer and altered the composites' thickness. Furthermore, due to the textiles' porous structure, the amount of biofilm integrated inside the textile matrix might not be reflected in the thickness of the composites, especially for the composites made with adsorption and vacuum filtration.

We showed that the biofilm-textile composites fabricated with the three methods effectively repaired mechanical damages by joining the ends of two 1 cm-wide composite pieces. The composites made with all three methods can be used as adhesive patches, and the performance of the self-repair depended on the cohesion strength between the two biofilm layers facing each other and the adhesion strength between the biofilm layer and the textile substrate. The single lap shear test results showed that the composites with doctor-bladed biofilm displayed comparable adhesion strengths in their lap joints regardless of their thicknesses. For the other two methods, we found that the adhesion strength of the lap joint increased with increasing integration density, as the adhesion was affected by the number of protruding textile fibers embedded in the biofilm layer. The more textile fibers the biofilm layer covered, the stronger the adhesion between the biofilm and the textile substrate. When the doctor-bladed composites were welded together, SEM showed that the cohesion occurred at the cross section of the biofilm layers on the two composite pieces. During the tensile tests, the position of the last crack closest to the cut indicated where the last

cohesion failure took place. This position then influenced the strength of the adhesion when the biofilm layer was peeled off from the textile substrate.

The biofilm-textile composites made with doctor blading demonstrated comparable adhesion strength (patching) and breaking stress (welding) to the composites doctor-bladed with untransformed bacterial cells, which did not produce curli fibers. Although mechanical test results appeared to undermine the role of curli in repairing the textiles, we have shown that doctor blading purified curli fibers was sufficient for patching-based self-repair. We also had a few hypotheses that can be validated with experiments in the future. First, we ended the culture expressing biofilms and the culture of untransformed cells when their OD600 reached ~4. In theory, both cultures should contain a comparable amount of cells and mass at this point, because 1) the two cultures had the same volume, 2) the *E. coli* strain we used lacks most of the EPS[104], and 3) water accounts for 70% of wet cell weight in *E. coli*[144]. However, after centrifugation at the same speed (4000×*g*) and for the same duration (25 min), the biofilm-expressing culture yielded ~30% more mass in the pellet than the culture of the untransformed cells. Whether the discrepancy of pellet mass solely resulted from the curli fibers expressed in the biofilm remained unclear for now, and can be elucidated in the future by counting the bacterial cell in the pellets and isolating and analyzing the curli fibers produced[145,146]. Second, we noticed that doctor blading cells and biofilms with the same wet thickness always led to a higher integration density of material in the cell composites than in the biofilm composites. We hypothesized that the cells were more compacted in the centrifuged pellets of untransformed cells compared to in the biofilm pellets, and a higher number of untransformed cells were doctor-bladed on textiles than the biofilm-expressing cells to achieve the same wet thickness. Manjula-Basavanna *et al.* pelleted the culture of the same *E. coli* strain, cast the pellet into films, and air-dried the material[120]. They imaged the cross section of the dry films

with FESEM and showed that the bacterial cells were deformed due to the dense packing[120]. Furthermore, the tight packing generated by centrifugal compaction and the drying process might have led to the damage of the cells and the release of cellular components, which might have played a role in the adhesion and cohesion of the cell coating in the textile composites[120,147]. The study of Manjula-Basavanna *et al.* revealed the ruptured cells on the surface of the dry films by FESEM imaging, a reduction of cell viability after the film fabrication by counting the colony forming units (CFU), and the amorphous heterogeneous composition by studying the films' physical and structural characteristics[120]. Therefore, quantifying the cell viability in both cultures after centrifugation and in the biofilm layer and the untransformed cell layer after doctor blading may provide helpful information, despite the fact that removing the adhesive cells completely from the textiles without damaging their integrity can be challenging[148]. If the centrifugal compaction was indeed higher for the untransformed cells compared to the cells embedded in extracellular curli fibers and caused more damage to the former, centrifuging the biofilm culture would yield a heavier pellet than pelleting the untransformed cell culture, with more cells remaining intact and precipitating, consistent with our previous observation. To understand the cell damage stemming from the centrifugal compaction, the centrifugation coefficient can be calculated for both cultures using the volume of a single *E. coli* cell, the number of cells in the pellet, and the volume of the pellet, as proposed by Peterson *et al.* [147]. The composition of the supernatant collected from both cultures after centrifugation can also be analyzed.

Future work can be done to exploit the living properties of biofilms in the biofilm-textile composites after the cell viability has been characterized. First, engineered curli fibers and other functional peptides can be expressed and secreted from the cells via the curli secretion pathway to modify the properties of biofilms as well as the composites. The stability of the functional biofilm

coating should be tested under various environmental conditions, such as different humidity levels, extreme temperatures, laundry, and long-term storage. Second, the reactivation of bacterial activities in the biofilm layer of the composites can be studied for the continuous expression of engineered curli fibers or functional peptides. In addition, the bacterial protein expression can be programmed to start after sensing certain environmental stimuli, such as temperature, pH, salt concentration, and mechanical tear, to enable more environmental-adaptive smart functions in the textile composites.

Compared to many non-biological self-repairing mechanisms developed, producing curli-expressing biofilms as repairing agents uses renewable feedstocks, permits biodegradation, and does not require hazardous chemicals or large amounts of polluting solvents. It is therefore in alignment with the principles of green chemistry[149]. Overall, this project has opened up new horizons for creating durable, sustainable, and multifunctional high-performance textiles with engineered living systems.

References

1 Bonaldi, R. R. in *High-Performance Apparel* (eds John McLoughlin & Tasneem Sabir) 129-156 (Woodhead Publishing, 2018).

2 McLoughlin, J. & Paul, R. in *High-Performance Apparel* (eds John McLoughlin & Tasneem Sabir) 223-244 (Woodhead Publishing, 2018).

3 Roy Choudhury, A. K. in *Principles of Textile Finishing* (ed Asim Kumar Roy Choudhury) 149-194 (Woodhead Publishing, 2017).

4 Holme, I. Innovative technologies for high performance textiles. *Coloration Technology* **123**, 59-73 (2007). https://doi.org/10.1111/j.1478-4408.2007.00064.x

5 Wang, H. *et al.* Durable, Self-Healing Superhydrophobic and Superoleophobic Surfaces from Fluorinated-Decyl Polyhedral Oligomeric Silsesquioxane and Hydrolyzed Fluorinated Alkyl Silane. *Angewandte Chemie International Edition* **50**, 11433-11436 (2011). https://doi.org/10.1002/anie.201105069

6 Gaddes, D. *et al.* Self-Healing Textile: Enzyme Encapsulated Layer-by-Layer Structural Proteins. *ACS Applied Materials & Interfaces* **8**, 20371-20378 (2016). https://doi.org/10.1021/acsami.6b05232

7 Ge, M. *et al.* A "PDMS-in-water" emulsion enables mechanochemically robust superhydrophobic surfaces with self-healing nature. *Nanoscale Horizons* **5**, 65-73 (2020). https://doi.org/10.1039/c9nh00519f

8 Liu, Y. *et al.* One-Step Modification of Fabrics with Bioinspired Polydopamine@Octadecylamine Nanocapsules for Robust and Healable Self-Cleaning Performance. *Small* **11**, 426-431 (2015). https://doi.org/10.1002/smll.201402383

9 Caschera, D. *et al.* Ultra Hydrophobic/Superhydrophilic Modified Cotton Textiles through Functionalized Diamond-Like Carbon Coatings for Self-Cleaning Applications. *Langmuir* **29**, 2775-2783 (2013). https://doi.org/10.1021/la305032k

10 Chen, J. *et al.* Nature-Inspired Hierarchical Protrusion Structure Construction for Washable and Wear-Resistant Superhydrophobic Textiles with Self-Cleaning Ability. *ACS Applied Materials & Interfaces* **13**, 18142-18151 (2021). https://doi.org/10.1021/acsami.1c03539

11 Yun, G. *et al.* Synthesis of Metal Nanoparticles in Metal-Phenolic Networks: Catalytic and Antimicrobial Applications of Coated Textiles. *Advanced Healthcare Materials* **7**, 1700934 (2018). https://doi.org/10.1002/adhm.201700934

12 Kwon, K. Y. *et al.* A Liquid Metal Mediated Metallic Coating for Antimicrobial and Antiviral Fabrics. *Adv Mater* **33**, 2104298 (2021). https://doi.org/10.1002/adma.202104298

13 Xu, A. Y., McGillivray, D. J. & Dingley, A. J. Active antibacterial coating of cotton fabrics with antimicrobial proteins. *Cellulose* **28**, 8077-8094 (2021). https://doi.org/10.1007/s10570-021-03997-2

14 Cao, Y.-M. *et al.* Smart Textiles Based on MoS2 Hollow Nanospheres for Personal Thermal Management. *ACS Applied Materials & Interfaces* **13**, 48988-48996 (2021). https://doi.org/10.1021/acsami.1c13269

15 Pakdel, E. *et al.* Superhydrophobic natural melanin-coated cotton with excellent UV protection and personal thermal management functionality. *Chemical Engineering Journal* **433**, 133688 (2022). https://doi.org/10.1016/j.cej.2021.133688

16 Wang, C. *et al.* Multifunctional wearable thermal management textile fabricated by one-step sputtering. *Nano Today* **45**, 101526 (2022). https://doi.org/10.1016/j.nantod.2022.101526

17 DeFrates, K. G. *et al.* Protein-Based Fiber Materials in Medicine: A Review. *Nanomaterials* **8**, 457 (2018). https://doi.org/10.3390/nano8070457

18 Keating, K. W. & Young, E. M. Synthetic biology for bio-derived structural materials. *Current Opinion in Chemical Engineering* **24**, 107-114 (2019). https://doi.org/10.1016/j.coche.2019.03.002

19 Nguyen, P. Q., Courchesne, N.-M. D., Duraj-Thatte, A., Praveschotinunt, P. & Joshi, N. S. Engineered Living Materials: Prospects and Challenges for Using Biological Systems to Direct the Assembly of Smart Materials. *Adv Mater* **30**, 1704847 (2018). https://doi.org/10.1002/adma.201704847

20 Gilbert, C. *et al.* Living materials with programmable functionalities grown from engineered microbial co-cultures. *Nat Mater* **20**, 691–700 (2021). https://doi.org/10.1038/s41563-020-00857-5

21 Sharma, G. *et al.* Escherichia coli biofilm: development and therapeutic strategies. *Journal of Applied Microbiology* **121**, 309-319 (2016). https://doi.org/10.1111/jam.13078

22 Jefferson, K. K. What drives bacteria to produce a biofilm? *FEMS Microbiology Letters* **236**, 163-173 (2004). https://doi.org/10.1111/j.1574-6968.2004.tb09643.x

23 Nguyen, P. Q. Synthetic biology engineering of biofilms as nanomaterials factories. *Biochemical Society Transactions* **45**, 585-597 (2017). https://doi.org/10.1042/bst20160348

24 Nordstedt, C. *et al.* The Alzheimer A beta peptide develops protease resistance in association with its polymerization into fibrils. *Journal of Biological Chemistry* **269**, 30773-30776 (1994). https://doi.org/10.1016/S0021-9258(18)47347-4

25 Schleeger, M. *et al.* Amyloids: From molecular structure to mechanical properties. *Polymer* **54**, 2473-2488 (2013). https://doi.org/10.1016/j.polymer.2013.02.029

26 Evans, M. L. & Chapman, M. R. Curli biogenesis: Order out of disorder. *Biochimica et Biophysica Acta (BBA) - Molecular Cell Research* **1843**, 1551-1558 (2014). https://doi.org/10.1016/j.bbamcr.2013.09.010

27 Collinson, S. K., Emödy, L., Müller, K. H., Trust, T. J. & Kay, W. W. Purification and characterization of thin, aggregative fimbriae from Salmonella enteritidis. *Journal of Bacteriology* **173**, 4773-4781 (1991). https://doi.org/10.1128/jb.173.15.4773-4781.1991

28 Zhong, C. *et al.* Strong underwater adhesives made by self-assembling multi-protein nanofibres. *Nature Nanotechnology* **9**, 858-866 (2014). https://doi.org/10.1038/nnano.2014.199

29 Dorval Courchesne, N.-M. *et al.* Biomimetic engineering of conductive curli protein films. *Nanotechnology* **29**, 454002 (2018). https://doi.org/10.1088/1361-6528/aadd3a

30 Saldanha, D. J., Abdali, Z., Modafferi, D., Janfeshan, B. & Dorval Courchesne, N.-M. Fabrication of fluorescent pH-responsive protein–textile composites. *Scientific Reports* **10**, 13052 (2020). https://doi.org/10.1038/s41598-020-70079-x

31 Abdali, Z. *et al.* Curli-Mediated Self-Assembly of a Fibrous Protein Scaffold for Hydroxyapatite Mineralization. *ACS Synthetic Biology* **9**, 3334-3343 (2020). https://doi.org/10.1021/acssynbio.0c00415

32 Nguyen, P. Q., Botyanszki, Z., Tay, P. K. R. & Joshi, N. S. Programmable biofilm-based materials from engineered curli nanofibres. *Nature Communications* **5**, 4945 (2014). https://doi.org/10.1038/ncomms5945

33 Kalyoncu, E., Ahan, R. E., Olmez, T. T. & Safak Seker, U. O. Genetically encoded conductive protein nanofibers secreted by engineered cells. *Rsc Adv* **7**, 32543-32551 (2017). https://doi.org/10.1039/C7RA06289C

34 Duraj-Thatte, A. M. *et al.* Genetically Programmable Self-Regenerating Bacterial Hydrogels. *Adv Mater* **31**, 1901826 (2019). https://doi.org/10.1002/adma.201901826

35 Wang, Y. *et al.* Living materials fabricated via gradient mineralization of light-inducible biofilms. *Nature Chemical Biology* **17**, 351-359 (2021). https://doi.org/10.1038/s41589-020-00697-z

36 Moser, F., Tham, E., González, L. M., Lu, T. K. & Voigt, C. A. Light-Controlled, High-Resolution Patterning of Living Engineered Bacteria Onto Textiles, Ceramics, and Plastic. *Adv Funct Mater* **29**, 1901788 (2019). https://doi.org/10.1002/adfm.201901788

37 Hemmatian, T., Lee, H. & Kim, J. Bacteria Adhesion of Textiles Influenced by Wettability and Pore Characteristics of Fibrous Substrates. *Polymers-Basel* **13**, 223 (2021). https://doi.org/10.3390/polym13020223

38 Travis, J. The naked truth?: Lice hint at a recent origin of clothing. *Science News* **164**, 118-118 (2003). https://doi.org/10.2307/3981931

39 Canavan, K. in *Textiles and Fashion* (ed Rose Sinclair) 531-545 (Woodhead Publishing, 2015).

40 de Oliveira, C. R. S., da Silva Júnior, A. H., Immich, A. P. S. & Fiates, J. Use of advanced materials in smart textile manufacturing. *Materials Letters* **316**, 132047 (2022). https://doi.org/10.1016/j.matlet.2022.132047

41 Shah, M. A., Pirzada, B. M., Price, G., Shibiru, A. L. & Qurashi, A. Applications of nanotechnology in smart textile industry: A critical review. *Journal of Advanced Research* **38**, 55-75 (2022). https://doi.org/10.1016/j.jare.2022.01.008

42 Liu, J. *et al.* Mechanically Robust and Flame-Retardant Superhydrophobic Textiles with Anti-Biofouling Performance. *Langmuir* **38**, 12961-12967 (2022). https://doi.org/10.1021/acs.langmuir.2c02248

43 He, W.-L. *et al.* Fabrication of P/N/B-Based Intumescent Flame-Retardant Coating for Polyester/Cotton Blend Fabric. *Materials* **15**, 6420 (2022). https://doi.org/10.3390/ma15186420

44 Das, P., Ganguly, S., Perelshtein, I., Margel, S. & Gedanken, A. Acoustic Green Synthesis of Graphene-Gallium Nanoparticles and PEDOT:PSS Hybrid Coating for Textile To Mitigate Electromagnetic Radiation Pollution. *ACS Applied Nano Materials* **5**, 1644-1655 (2022). https://doi.org/10.1021/acsanm.1c04425

45 Alam, T., Saidane, F., Faisal, A. a., Khan, A. & Hossain, G. Smart- textile strain sensor for human joint monitoring. *Sensors and Actuators A: Physical* **341**, 113587 (2022). https://doi.org/10.1016/j.sna.2022.113587

46 Arat, R., Jia, G. & Plentz, J. Wet chemical method for highly flexible and conductive fabrics for smart textile applications. *The Journal of The Textile Institute*, 1-6 (2022). https://doi.org/10.1080/00405000.2022.2061760

47 Hossain, I. Z., Khan, A. & Hossain, G. A Piezoelectric Smart Textile for Energy Harvesting and Wearable Self-Powered Sensors. *Energies* **15**, 5541 (2022). https://doi.org/10.3390/en15155541

48 Botta, V. Durable, repairable and mainstream - How ecodesign can make our textiles circular. (2021).

49 EEA. Textiles and the environment: the role of design in Europe's circular economy. *EEA Briefing Fe 10/2020, European Environment Agency* (2022). https://doi.org/10.2800/006659

50 Bick, R., Halsey, E. & Ekenga, C. C. The global environmental injustice of fast fashion. *Environmental Health* **17**, 92 (2018). https://doi.org/10.1186/s12940-018-0433-7

51 Chen, X., Memon, H. A., Wang, Y., Marriam, I. & Tebyetekerwa, M. Circular Economy and Sustainability of the Clothing and Textile Industry. *Materials Circular Economy* **3**, 12 (2021). https://doi.org/10.1007/s42824-021-00026-2

52 Niinimäki, K. *et al.* The environmental price of fast fashion. *Nature Reviews Earth & Environment* **1**, 189-200 (2020). https://doi.org/10.1038/s43017-020-0039-9

53 European Union. EU Strategy for Sustainable and Circular Textiles. (2022).

54 Ramesh, S. *et al.* Self-healing and repair of fabrics: A comprehensive review of the application toolkit. *Materials Today* **54**, 90-109 (2022). https://doi.org/10.1016/j.mattod.2021.11.016

55 Li, Y. *et al.* Intelligent self-healing superhydrophobic modification of cotton fabrics via surface-initiated ARGET ATRP of styrene. *Chemical Engineering Journal* **323**, 134-142 (2017). https://doi.org/10.1016/j.cej.2017.04.080

56 Zhou, H., Wang, H., Niu, H., Gestos, A. & Lin, T. Robust, Self-Healing Superamphiphobic Fabrics Prepared by Two-Step Coating of Fluoro-Containing Polymer, Fluoroalkyl Silane, and Modified Silica Nanoparticles. *Adv Funct Mater* **23**, 1664-1670 (2013). https://doi.org/10.1002/adfm.201202030

57 Ryu, Y. S., Oh, K. W. & Kim, S. H. Furan-based self-healing breathable elastomer coating on polylactide fabric. *Textile Research Journal* **89**, 814-824 (2019). https://doi.org/10.1177/0040517518755791

58 Ramesh, S. *et al.* Dual-Responsive Microgels for Structural Repair and Recovery of Nonwoven Membranes for Liquid Filtration. *ACS Applied Polymer Materials* **3**, 1508-1517 (2021). https://doi.org/10.1021/acsapm.0c01360

59 Zhou, H., Wang, H., Niu, H. & Lin, T. Recent Progress in Durable and Self-Healing Super-Nonwettable Fabrics. *Advanced Materials Interfaces* **5**, 1800461 (2018). https://doi.org/10.1002/admi.201800461

60 Wang, H., Zhou, H., Gestos, A., Fang, J. & Lin, T. Robust, Superamphiphobic Fabric with Multiple Self-Healing Ability against Both Physical and Chemical Damages. *ACS Applied Materials & Interfaces* **5**, 10221-10226 (2013). https://doi.org/10.1021/am4029679

61 Wang, H. *et al.* Robust, electro-conductive, self-healing superamphiphobic fabric prepared by one-step vapour-phase polymerisation of poly(3,4-ethylenedioxythiophene) in the presence of fluorinated decyl polyhedral oligomeric silsesquioxane and fluorinated alkyl silane. *Soft Matter* **9**, 277-282 (2013). https://doi.org/10.1039/C2SM26871J

62 Qiang, S., Chen, K., Yin, Y. & Wang, C. Robust UV-cured superhydrophobic cotton fabric surfaces with self-healing ability. *Materials & Design* **116**, 395-402 (2017). https://doi.org/10.1016/j.matdes.2016.11.099

63 Li, B. & Zhang, J. Durable and self-healing superamphiphobic coatings repellent even to hot liquids. *Chemical Communications* **52**, 2744-2747 (2016). https://doi.org/10.1039/C5CC09951J

64 Xue, C.-H., Bai, X. & Jia, S.-T. Robust, Self-Healing Superhydrophobic Fabrics Prepared by One-Step Coating of PDMS and Octadecylamine. *Scientific Reports* **6**, 27262 (2016). https://doi.org/10.1038/srep27262

65 Zhou, F. *et al.* Fabrication of robust and self-healing superhydrophobic PET fabrics based on profiled fiber structure. *Colloids and Surfaces A: Physicochemical and Engineering Aspects* **609**, 125686 (2021). https://doi.org/10.1016/j.colsurfa.2020.125686

66 Xu, Q. *et al.* Superhydrophobic cotton fabric with excellent healability fabricated by the "grafting to" method using a diblock copolymer mist. *Chemical Engineering Journal* **379**, 122401 (2020). https://doi.org/10.1016/j.cej.2019.122401

67 Li, D. & Guo, Z. Stable and self-healing superhydrophobic MnO2@fabrics: Applications in self-cleaning, oil/water separation and wear resistance. *Journal of Colloid and Interface Science* **503**, 124-130 (2017). https://doi.org/10.1016/j.jcis.2017.05.015

68 Lindstrom, A. B., Strynar, M. J. & Libelo, E. L. Polyfluorinated Compounds: Past, Present, and Future. *Environmental Science & Technology* **45**, 7954-7961 (2011). https://doi.org/10.1021/es2011622

69 Li, Y., Ge, B., Men, X., Zhang, Z. & Xue, Q. A facile and fast approach to mechanically stable and rapid self-healing waterproof fabrics. *Composites Science and Technology* **125**, 55-61 (2016). https://doi.org/10.1016/j.compscitech.2016.01.021

70 Zhou, H. *et al.* Superstrong, Chemically Stable, Superamphiphobic Fabrics from Particle-Free Polymer Coatings. *Advanced Materials Interfaces* **2**, 1400559 (2015). https://doi.org/10.1002/admi.201400559

71 Saldanha, D. J., Cai, A. & Dorval Courchesne, N.-M. The Evolving Role of Proteins in Wearable Sweat Biosensors. *ACS Biomaterials Science & Engineering* (2021). https://doi.org/10.1021/acsbiomaterials.1c00699

72 Wilson, K. *A history of textiles*. (Routledge, 2021).

73 Numata, K. How to define and study structural proteins as biopolymer materials. *Polymer Journal* **52**, 1043-1056 (2020). https://doi.org/10.1038/s41428-020-0362-5

74 Guerette, P. A. *et al.* Nanoconfined β-Sheets Mechanically Reinforce the Supra-Biomolecular Network of Robust Squid Sucker Ring Teeth. *ACS Nano* **8**, 7170-7179 (2014). https://doi.org/10.1021/nn502149u

75 Miserez, A. *et al.* Microstructural and Biochemical Characterization of the Nanoporous Sucker Rings from Dosidicus gigas. *Adv Mater* **21**, 401-406 (2009). https://doi.org/10.1002/adma.200801197

76 Pena-Francesch, A. *et al.* Mechanical Properties of Tandem-Repeat Proteins Are Governed by Network Defects. *ACS Biomaterials Science & Engineering* **4**, 884-891 (2018). https://doi.org/10.1021/acsbiomaterials.7b00830

77 Pena-Francesch, A. & Demirel, M. C. Squid-Inspired Tandem Repeat Proteins: Functional Fibers and Films. *Frontiers in Chemistry* **7** (2019). https://doi.org/10.3389/fchem.2019.00069

78 Sariola, V. *et al.* Segmented molecular design of self-healing proteinaceous materials. *Scientific Reports* **5**, 13482 (2015). https://doi.org/10.1038/srep13482

79 Ding, D. *et al.* Biomimetic Production of Silk-Like Recombinant Squid Sucker Ring Teeth Proteins. *Biomacromolecules* **15**, 3278-3289 (2014). https://doi.org/10.1021/bm500670r

80 Cappello, J. *et al.* Genetic engineering of structural protein polymers. *Biotechnol Prog* **6**, 198-202 (1990). https://doi.org/10.1021/bp00003a006

81 Mozhdehi, D., Luginbuhl, K. M., Roberts, S. & Chilkoti, A. in *Sequence-Controlled Polymers* 91-115 (Wiley-VCH, 2018).

82 Charrier, M. *et al.* Engineering high-yield biopolymer secretion creates an extracellular protein matrix for living materials. *mSystems* **6**, e00903-00920 (2020). https://doi.org/10.1101/2020.08.31.276303

83 Chen, A. Y., Zhong, C. & Lu, T. K. Engineering Living Functional Materials. *ACS Synthetic Biology* **4**, 8-11 (2015). https://doi.org/10.1021/sb500113b

84 Branda, S. S., Vik, Å., Friedman, L. & Kolter, R. Biofilms: the matrix revisited. *Trends in Microbiology* **13**, 20-26 (2005). https://doi.org/10.1016/j.tim.2004.11.006

85 Vishwakarma, V. Impact of environmental biofilms: Industrial components and its remediation. *Journal of Basic Microbiology* **60**, 198-206 (2020). https://doi.org/10.1002/jobm.201900569

86 Møllebjerg, A., Palmén, L. G., Gori, K. & Meyer, R. L. The Bacterial Life Cycle in Textiles is Governed by Fiber Hydrophobicity. *Microbiology Spectrum* **9**, e01185-01121 (2021). https://doi.org/10.1128/Spectrum.01185-21

87 Raab, N. *et al.* A symbiotic-like biologically-driven regenerating fabric. *Scientific Reports* **7**, 8528 (2017). https://doi.org/10.1038/s41598-017-09105-4

88 Wang, W. *et al.* Harnessing the hygroscopic and biofluorescent behaviors of genetically tractable microbial cells to design biohybrid wearables. *Science Advances* **3**, e1601984 (2017). https://doi.org/10.1126/sciadv.1601984

89 Tenaillon, O., Skurnik, D., Picard, B. & Denamur, E. The population genetics of commensal Escherichia coli. *Nature Reviews Microbiology* **8**, 207-217 (2010). https://doi.org/10.1038/nrmicro2298

90 Probert, H. M. & Gibson, G. R. Bacterial biofilms in the human gastrointestinal tract. *Current issues in intestinal microbiology* **3**, 23-27 (2002).

91 Beloin, C., Roux, A. & Ghigo, J.-M. in *Bacterial Biofilms* (ed Tony Romeo) 249-289 (Springer Berlin Heidelberg, 2008).

92 Pratt, L. A. & Kolter, R. Genetic analysis of Escherichia coli biofilm formation: roles of flagella, motility, chemotaxis and type I pili. *Molecular Microbiology* **30**, 285-293 (1998). https://doi.org/10.1046/j.1365-2958.1998.01061.x

93 Tursi, S. A. & Tükel, Ç. Curli-Containing Enteric Biofilms Inside and Out: Matrix Composition, Immune Recognition, and Disease Implications. *Microbiology and Molecular Biology Reviews* **82**, e00028-00018 (2018). https://doi.org/10.1128/MMBR.00028-18

94 Serra, D. O., Richter, A. M. & Hengge, R. Cellulose as an Architectural Element in Spatially Structured Escherichia coli Biofilms. *Journal of Bacteriology* **195**, 5540-5554 (2013). https://doi.org/10.1128/JB.00946-13

95 Gualdi, L. *et al.* Cellulose modulates biofilm formation by counteracting curli-mediated colonization of solid surfaces in Escherichia coli. *Microbiology* **154**, 2017-2024 (2008). https://doi.org/10.1099/mic.0.2008/018093-0

96 Barnhart, M. M. & Chapman, M. R. Curli biogenesis and function. *Annu Rev Microbiol* **60**, 131-147 (2006). https://doi.org/10.1146/annurev.micro.60.080805.142106

97 DeBenedictis, E. P., Liu, J. & Keten, S. Adhesion mechanisms of curli subunit CsgA to abiotic surfaces. *Science Advances* **2**, e1600998 (2016). https://doi.org/10.1126/sciadv.1600998

98 Chapman, M. R. *et al.* Role of Escherichia coli Curli Operons in Directing Amyloid Fiber Formation. *Science* **295**, 851-855 (2002). https://doi.org/10.1126/science.1067484

99 Hammar, M., Bian, Z. & Normark, S. Nucleator-dependent intercellular assembly of adhesive curli organelles in Escherichia coli. *Proceedings of the National Academy of Sciences* **93**, 6562-6566 (1996). https://doi.org/10.1073/pnas.93.13.6562

100 Abdali, Z. *et al.* Extracellular Secretion and Simple Purification of Bacterial Collagen from Escherichia coli. *Biomacromolecules* **23**, 1557-1568 (2022). https://doi.org/10.1021/acs.biomac.1c01191

101 Shewmaker, F. *et al.* The Functional Curli Amyloid Is Not Based on In-register Parallel β-Sheet Structure*. *Journal of Biological Chemistry* **284**, 25065-25076 (2009). https://doi.org/10.1074/jbc.M109.007054

102 Sleutel, M., Pradhan, B. & Remaut, H. Structural analysis of the bacterial amyloid curli. *bioRxiv* (2022). https://doi.org/10.1101/2022.02.28.482343

103 Appel, T. R., Wolff, M., von Rheinbaben, F., Heinzel, M. & Riesner, D. Heat stability of prion rods and recombinant prion protein in water, lipid and lipid–water mixtures. *Journal of General Virology* **82**, 465-473 (2001). https://doi.org/10.1099/0022-1317-82-2-465

104 Tay, P. K. R., Nguyen, P. Q. & Joshi, N. S. A Synthetic Circuit for Mercury Bioremediation Using Self-Assembling Functional Amyloids. *ACS Synthetic Biology* **6**, 1841-1850 (2017). https://doi.org/10.1021/acssynbio.7b00137

105 Pesavento, C. *et al.* Inverse regulatory coordination of motility and curli-mediated adhesion in Escherichia coli. *Genes Dev* **22**, 2434-2446 (2008). https://doi.org/10.1101/gad.475808

106 Duraj-Thatte, A. M. *et al.* Water-processable, biodegradable and coatable aquaplastic from engineered biofilms. *Nature Chemical Biology* **17**, 732-738 (2021). https://doi.org/10.1038/s41589-021-00773-y

107 Dorval Courchesne, N.-M., Duraj-Thatte, A., Tay, P. K. R., Nguyen, P. Q. & Joshi, N. S. Scalable Production of Genetically Engineered Nanofibrous Macroscopic Materials via Filtration. *ACS Biomaterials Science & Engineering* **3**, 733-741 (2017). https://doi.org/10.1021/acsbiomaterials.6b00437

108 Duraj-Thatte, A. M. *et al.* Modulating bacterial and gut mucosal interactions with engineered biofilm matrix proteins. *Scientific Reports* **8**, 3475 (2018). https://doi.org/10.1038/s41598-018-21834-8

109 Huyer, C. *et al.* Fabrication of Curli Fiber-PEDOT:PSS Biomaterials with Tunable Self-Healing, Mechanical, and Electrical Properties. *ACS Biomaterials Science & Engineering* (2022). https://doi.org/10.1021/acsbiomaterials.1c01180

110 Jean, L., Foley, A. C. & Vaux, D. J. T. The Physiological and Pathological Implications of the Formation of Hydrogels, with a Specific Focus on Amyloid Polypeptides. *Biomolecules* **7**, 70 (2017). https://doi.org/10.3390/biom7040070

111 Toksoz, S., Acar, H. & Guler, M. O. Self-assembled one-dimensional soft nanostructures. *Soft Matter* **6**, 5839-5849 (2010). https://doi.org/10.1039/C0SM00121J

112 Stephanopoulos, N., Ortony, J. H. & Stupp, S. I. Self-assembly for the synthesis of functional biomaterials. *Acta Mater* **61**, 912-930 (2013). https://doi.org/10.1016/j.actamat.2012.10.046

113 Branco, M. C., Nettesheim, F., Pochan, D. J., Schneider, J. P. & Wagner, N. J. Fast Dynamics of Semiflexible Chain Networks of Self-Assembled Peptides. *Biomacromolecules* **10**, 1374-1380 (2009). https://doi.org/10.1021/bm801396e

114 Ghouri, A. S., Aslam, R., Siddiqui, M. S. & Sami, S. K. Recent Progress in Textile-Based Flexible Supercapacitor. *Front Mater* **7** (2020). https://doi.org/10.3389/fmats.2020.00058

115 Bandodkar, A. J., Jeerapan, I. & Wang, J. Wearable Chemical Sensors: Present Challenges and Future Prospects. *Acs Sensors* **1**, 464-482 (2016). https://doi.org/10.1021/acssensors.6b00250

116 Mukhopadhyay, A. & Midha, V. K. A Review on Designing the Waterproof Breathable Fabrics Part I: Fundamental Principles and Designing Aspects of Breathable Fabrics. *Journal of Industrial Textiles* **37**, 225-262 (2008). https://doi.org/10.1177/1528083707082164

117 Morshed, M. N., Behary, N., Bouazizi, N., Guan, J. & Nierstrasz, V. A. An overview on biocatalysts immobilization on textiles: Preparation, progress and application in wastewater treatment. *Chemosphere* **279**, 130481 (2021). https://doi.org/10.1016/j.chemosphere.2021.130481

118 Kiehl, K., Straube, T., Opwis, K. & Gutmann, J. S. Strategies for permanent immobilization of enzymes on textile carriers. *Engineering in Life Sciences* **15**, 622-626 (2015). https://doi.org/10.1002/elsc.201400148

119 Axpe, E. *et al.* Fabrication of Amyloid Curli Fibers–Alginate Nanocomposite Hydrogels with Enhanced Stiffness. *ACS Biomaterials Science & Engineering* **4**, 2100-2105 (2018). https://doi.org/10.1021/acsbiomaterials.8b00364

120 Manjula-Basavanna, A., Duraj-Thatte, A. M. & Joshi, N. S. Robust Self-Regeneratable Stiff Living Materials Fabricated from Microbial Cells. *Adv Funct Mater* **31**, 2010784 (2021). https://doi.org/10.1002/adfm.202010784

121 Carniello, V., Peterson, B. W., van der Mei, H. C. & Busscher, H. J. Physico-chemistry from initial bacterial adhesion to surface-programmed biofilm growth. *Advances in Colloid and Interface Science* **261**, 1-14 (2018). https://doi.org/10.1016/j.cis.2018.10.005

122 Hermansson, M. The DLVO theory in microbial adhesion. *Colloids and Surfaces B: Biointerfaces* **14**, 105-119 (1999). https://doi.org/10.1016/S0927-7765(99)00029-6

123 Olsson, A. L., van der Mei Hc Fau - Busscher, H. J., Busscher Hj Fau - Sharma, P. K. & Sharma, P. K. Novel analysis of bacterium-substratum bond maturation measured using a quartz crystal microbalance. *Langmuir* **26**, 11113–11117 https://doi.org/10.1021/la100896a

124 Cookson, A. L., Cooley, W. A. & Woodward, M. J. The role of type 1 and curli fimbriae of Shiga toxin-producing Escherichia coli in adherence to abiotic surfaces. *International Journal of Medical Microbiology* **292**, 195-205 (2002). https://doi.org/10.1078/1438-4221-00203

125 Vidal, O. *et al.* Isolation of an Escherichia coli K-12 Mutant Strain Able To Form Biofilms on Inert Surfaces: Involvement of a New ompR Allele That Increases Curli Expression. *Journal of Bacteriology* **180**, 2442-2449 (1998). https://doi.org/10.1128/JB.180.9.2442-2449.1998

126 Tang, X. & Yan, X. Dip-coating for fibrous materials: mechanism, methods and applications. *Journal of Sol-Gel Science and Technology* **81**, 378-404 (2017). https://doi.org/10.1007/s10971-016-4197-7

127 Garrett, T. R., Bhakoo, M. & Zhang, Z. Bacterial adhesion and biofilms on surfaces. *Progress in Natural Science* **18**, 1049-1056 (2008). https://doi.org/10.1016/j.pnsc.2008.04.001

128 Kabir, S. M. F. & Haque, S. A Mini Review on the Innovations in Sizing of Cotton. *Journal of Natural Fibers* **19**, 6993–7007 (2022). https://doi.org/10.1080/15440478.2021.1941486

129 Krykpayev, B., Farooqui, M. F., Bilal, R. M., Vaseem, M. & Shamim, A. A wearable tracking device inkjet-printed on textile. *Microelectronics Journal* **65**, 40-48 (2017). https://doi.org/10.1016/j.mejo.2017.05.010

130 Song, J., Gao, L., Tao, X. & Li, L. Ultra-Flexible and Large-Area Textile-Based Triboelectric Nanogenerators with a Sandpaper-Induced Surface Microstructure. *Materials* **11**, 2120 (2018). https://doi.org/10.3390/ma11112120

131 Deng, Y. *et al.* Scalable fabrication of efficient organolead trihalide perovskite solar cells with doctor-bladed active layers. *Energy & Environmental Science* **8**, 1544-1550 (2015). https://doi.org/10.1039/C4EE03907F

132 Hu, Q. *et al.* Large-area perovskite nanowire arrays fabricated by large-scale roll-to-roll micro-gravure printing and doctor blading. *Nanoscale* **8**, 5350-5357 (2016). https://doi.org/10.1039/C5NR08277C

133 Tsurko, E. S. *et al.* Large Scale Self-Assembly of Smectic Nanocomposite Films by Doctor Blading versus Spray Coating: Impact of Crystal Quality on Barrier Properties. *Macromolecules* **50**, 4344-4350 (2017). https://doi.org/10.1021/acs.macromol.7b00701

134 Sivanathan, V. & Hochschild, A. Generating extracellular amyloid aggregates using E. coli cells. *Genes Dev* **26**, 2659-2667 (2012). https://doi.org/10.1101/gad.205310.112

135 Sivanathan, V. & Hochschild, A. A bacterial export system for generating extracellular amyloid aggregates. *Nat Protoc* **8**, 1381-1390 (2013). https://doi.org/10.1038/nprot.2013.081

136 Li, C., Adamcik, J. & Mezzenga, R. Biodegradable nanocomposites of amyloid fibrils and graphene with shape-memory and enzyme-sensing properties. *Nature Nanotechnology* **7**, 421-427 (2012). https://doi.org/10.1038/nnano.2012.62

137 Li, C., Bolisetty, S. & Mezzenga, R. Hybrid Nanocomposites of Gold Single-Crystal Platelets and Amyloid Fibrils with Tunable Fluorescence, Conductivity, and Sensing Properties. *Adv Mater* **25**, 3694-3700 (2013). https://doi.org/10.1002/adma.201300904

138 Li, C. *et al.* Amyloid-Hydroxyapatite Bone Biomimetic Composites. *Adv Mater* **26**, 3207-3212 (2014). https://doi.org/10.1002/adma.201306198

139 Ling, S. *et al.* Modulating Materials by Orthogonally Oriented β-Strands: Composites of Amyloid and Silk Fibroin Fibrils. *Adv Mater* **26**, 4569-4574 (2014). https://doi.org/10.1002/adma.201400730

140 Bolisetty, S., Arcari, M., Adamcik, J. & Mezzenga, R. Hybrid Amyloid Membranes for Continuous Flow Catalysis. *Langmuir* **31**, 13867-13873 (2015). https://doi.org/10.1021/acs.langmuir.5b03205

141 Peng, X., Jin, J., Ericsson, E. M. & Ichinose, I. General Method for Ultrathin Free-Standing Films of Nanofibrous Composite Materials. *Journal of the American Chemical Society* **129**, 8625-8633 (2007). https://doi.org/10.1021/ja0718974

142 Adolphe, D. C. & Dolez, P. I. in *Advanced Characterization and Testing of Textiles* (eds Patricia Dolez, Olivier Vermeersch, & Valério Izquierdo) 25-57 (Woodhead Publishing, 2018).

143 Li, X., Li, Y., Guan, T., Xu, F. & Sun, J. Durable, Highly Electrically Conductive Cotton Fabrics with Healable Superamphiphobicity. *ACS Applied Materials & Interfaces* **10**, 12042-12050 (2018). https://doi.org/10.1021/acsami.8b01279

144 Feijó Delgado, F. *et al.* Intracellular Water Exchange for Measuring the Dry Mass, Water Mass and Changes in Chemical Composition of Living Cells. *PLOS ONE* **8**, e67590 (2013). https://doi.org/10.1371/journal.pone.0067590

145 Van Gerven, N. *et al.* Secretion and functional display of fusion proteins through the curli biogenesis pathway. *Molecular Microbiology* **91**, 1022-1035 (2014). https://doi.org/10.1111/mmi.12515

146 Dueholm, M. S. *et al.* Expression of Fap amyloids in Pseudomonas aeruginosa, P. fluorescens, and P. putida results in aggregation and increased biofilm formation. *MicrobiologyOpen* **2**, 365-382 (2013). https://doi.org/10.1002/mbo3.81

147 Peterson, B. W., Sharma, P. K., Mei, H. C. v. d. & Busscher, H. J. Bacterial Cell Surface Damage Due to Centrifugal Compaction. *Applied and Environmental Microbiology* **78**, 120-125 (2012). https://doi.org/10.1128/AEM.06780-11

148 Hemmatian, T. & Kim, J. Quantification Methods for Textile-Adhered Bacteria: Extraction, Colorimetric, and Microscopic Analysis. *Polymers-Basel* **11**, 1666 (2019). https://doi.org/10.3390/polym11101666

149 Anastas, P. T. & Warner, J. C. *Green chemistry : theory and practice*. xi, 135 pages ; 23 cm (Oxford University Press, 1998).

Appendices

Appendix A: Biofilm-textile Composites Fabrication

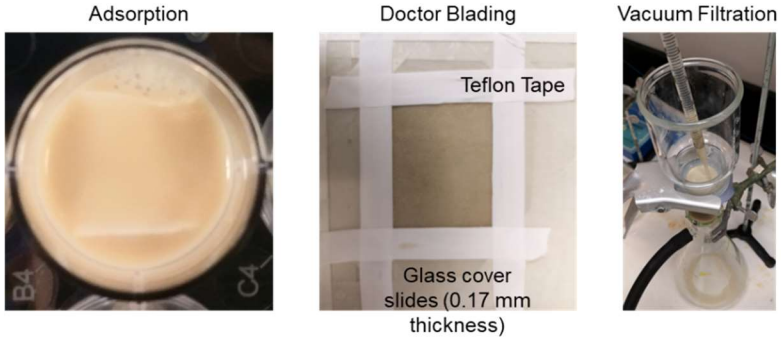

Images of fabricating biofilm-textile composites by incubating the textiles in biofilm solutions (adsorption, left), spreading biofilm pellets on textiles using glass cover slides as masks and blade (doctor blading, middle), and vacuum filtering a concentrated biofilm solution through textile (vacuum filtration, right).

Appendix B: Mechanical Test Setup and Data Analysis

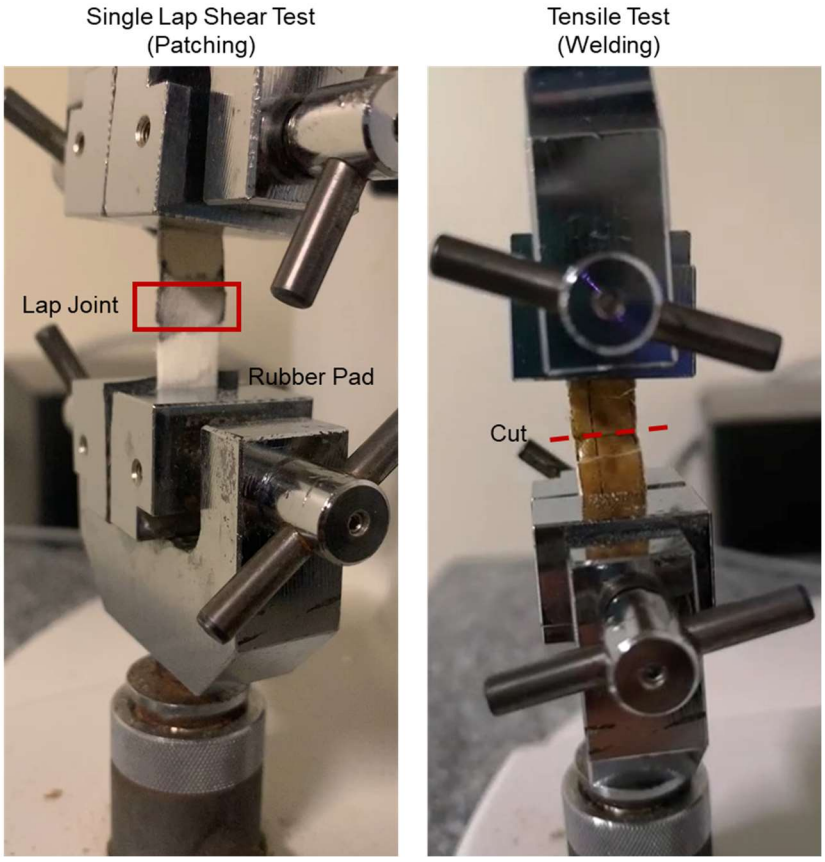

Images showing the setup of the single lap shear test done with the patched composites (prepared by doctor blading purified curli fibers on textiles) and the tensile test done with the welded composites (prepared by doctor blading curli biofilm on textiles). The red box on the left image indicates the lap joint. The red dashed line on the right image showed the linear cut created by scissors and repaired. To increase the grip and prevent the textile composites from slipping off from the metal grips of the tensile tester, a rubber pad was added between the specimen and the metal grip.

A MATLAB script (shown below) was created to process the data from the tensile tests, calculate the stress and strain values, and plot the stress-strain curve of individual specimens and the average curve for replicates. The script generates stress-strain curves in the MATLAB figure format (.fig) and Portable Network Graphics format (.png).

```
%%%%%%%%%%%%%%%%%%%%%%%%%%%%%%%%%%%%%%%%%%%%%%%%%%%%%%%%%%%%%%%%%%%%%%%%%%%%
%                          DORVAL LAB                                        %
%                          AUTHOR: ANQI CAI                                  %
%                          V1.0, NOVEMBER 2, 2020                            %
%    THIS SCRIPT PLOTS THE STRESS-STRAIN CURVES FROM TENSILE TESTS           %
%%%%%%%%%%%%%%%%%%%%%%%%%%%%%%%%%%%%%%%%%%%%%%%%%%%%%%%%%%%%%%%%%%%%%%%%%%%%

%%
clear;
clc;
close all;

%%
%%%%%%%%%%%%%%%%%%%%%%%%%%%%%%%%%%%%%%%%%%%%%%%%%%%%%%%%%%%%%%%%%%%%%%%%%%%%
%                  CHANGE DIRECTORY HERE                                     %
%%%%%%%%%%%%%%%%%%%%%%%%%%%%%%%%%%%%%%%%%%%%%%%%%%%%%%%%%%%%%%%%%%%%%%%%%%%%
cd('.\Research\Data\Tensile Test\Mar 01 2021');
if ~exist('plots', 'dir')
    mkdir('plots');
end

%% File setup
%%%%%%%%%%%%%%%%%%%%%%%%%%%%%%%%%%%%%%%%%%%%%%%%%%%%%%%%%%%%%%%%%%%%%%%%%%%%
%                  CHANGE FILE NAME HERE                                     %
%%%%%%%%%%%%%%%%%%%%%%%%%%%%%%%%%%%%%%%%%%%%%%%%%%%%%%%%%%%%%%%%%%%%%%%%%%%%
filename = '20210301_AC_Healing.xlsx';
% Obtain xls sheet info
[~, sheets] = xlsfinfo(filename);
sampleNames = cell(1, length(sheets));

% Store averages of each sheet
% 1st line: stress, 2nd line: strain
stress_strain_ave = cell(2, length(sheets));

for i = 1:length(sheets)
    [data, text, raw] = xlsread(filename, sheets{i});

    % Detect how many specimen are specified in this sheet
    n_specimen = 0;
    for j = 4:size(data, 1)
        if ~isnan(data(j, 2))
            n_specimen = n_specimen + 1;
        else
            break;
        end
    end

    %% Read specimen information from xls sheet
    widths = zeros(1, n_specimen);
    thicknesses = zeros(1, n_specimen);
    GLs = zeros(1, n_specimen);

    for j = 1:n_specimen
        widths(j) = data(4+j-1, 2);
        thicknesses(j) = data(4+j-1, 3);
```

```
        GLs(j) = data(4+j-1, 4);
    end

    %% Find the starting index of the specimens.
    % First line is the starting index
    % Second line is the ending index
    % Third line is the length
    indices = zeros(3, n_specimen);
    for j = 1:n_specimen
        tag = ['Specimen  1' ' - ' num2str(j)];
        indices(1, j) = find(strcmp(raw, tag)) + 3 - 1; % Starting index of the
current specimen in DATA

        if j ~= 1
            indices(2, j - 1) = find(strcmp(raw, tag)) - 3 - 1; % Calculate ending
index of the previous specimen in DATA
            indices(3, j - 1) = indices(2, j - 1) - indices(1, j - 1) + 1; %
Calculate the length of the previous specimen
        end
        if j == n_specimen
            indices(2, j) = size(data, 1);
            indices(3, j) = indices(2, j) - indices(1, j) + 1;
        end
    end

    % Store the stress & strain data of the specimens
    stress = cell(1, n_specimen);
    strain = cell(1, n_specimen);

    % Store the average of specimen stress & strain data
    stress_ave = zeros(1, max(indices(3,:)));
    strain_ave = zeros(1, max(indices(3,:)));
    counter = zeros(1, max(indices(3, :))); % Count the number of data points

    for j = 1:n_specimen
        load = data(indices(1,j):indices(2,j), 2);
        pos = data(indices(1,j):indices(2,j), 3);

        % Calculate stress & strain.
        for k = 1:length(load)
            stress_sample = load(k) / (widths(j) * thicknesses(j));
            strain_sample = 100 * pos(k) / GLs(j);

            stress{j}(k) = stress_sample;
            strain{j}(k) = strain_sample;

            stress_ave(k) = stress_ave(k) + stress_sample;
            strain_ave(k) = strain_ave(k) + strain_sample;
            counter(k) = counter(k) + 1;
        end
    end
    stress_strain_ave{1, i} = stress_ave ./ counter;
    stress_strain_ave{2, i} = strain_ave ./ counter;

    % Replace all SPACE and UNDERSCORE in sample name into '\_'
```

```
    sampleNames{i} = strrep(raw{2, 1}, '_', '\_');
    sampleNames{i} = strrep(sampleNames{i}, ' ', '\_');
    fig_stress_strain = figure;
    hold on;
    grid on;
    title(['Sheet ' num2str(i) ': Stress Strain Plot of ' sampleNames{i}]);
    xlabel('Strain (%)');
    ylabel('Stress (MPa)');
    ylim([0 inf])
    for j = 1:length(stress)
        plot(strain{j}, stress{j});
    end

    if ~exist('./plots/fig', 'dir')
        mkdir('./plots/fig');
    end
    if ~exist('./plots/png', 'dir')
        mkdir('./plots/png');
    end
    savefig(fig_stress_strain, strcat('./plots/fig/Sheet_', num2str(i), '_',
strrep(sampleNames{i}, '\_', '_'), '_Stress_Strain'));
    saveas(fig_stress_strain, strcat('./plots/png/Sheet_', num2str(i), '_',
strrep(sampleNames{i}, '\_', '_'), '_Stress_Strain'), 'png');
    close(fig_stress_strain);

    % Process the average
end

% Plot stress strain average
fig_stress_strain_ave = figure;
hold on;
grid on;
title('Average Stress Strain Curve');
xlabel('Strain (%)');
ylabel('Stress (MPa)');

for i = 1:length(sheets)
    plot(stress_strain_ave{2, i}, stress_strain_ave{1, i});
end
legend(sampleNames{:}, 'location', 'northwest');
savefig(fig_stress_strain_ave, strcat('./plots/fig/Average_', num2str(i), '_',
strrep(sampleNames{i}, '\_', '_'), '_Stress_Strain'));
saveas(fig_stress_strain_ave, strcat('./plots/png/Average_', num2str(i), '_',
strrep(sampleNames{i}, '\_', '_'), '_Stress_Strain'), 'png');
close(fig_stress_strain_ave);
```

Appendix C: Elongation at Break in Tensile Tests

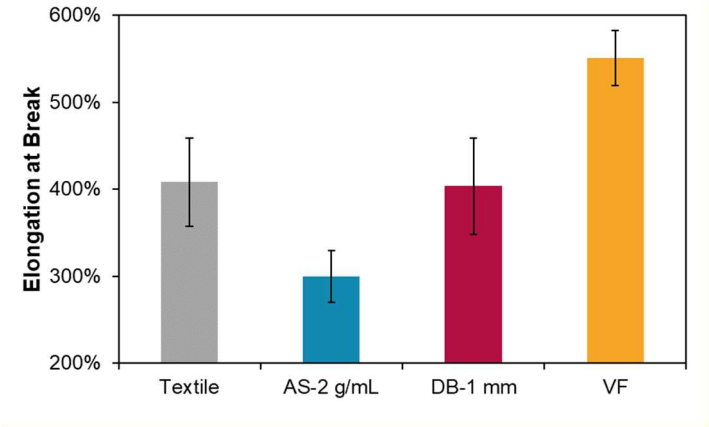

Bar plot of the elongation at break obtained from the tesile test results of the plain textiles and biofilm-textile composites. Vacuum filtering a layer of biofilm on textiles increased the textiles' extensibility before mechanical failure. The bars represent mean values, and the error bars are standard deviations.